Dyonic Lieb-Schultz-Mattis theorem and symmetry protected topological phases in decorated dimer models

Xu Yang, Shenghan Jiang, Ashvin Vishwanath, and Ying Ran

Phys. Rev. B **98**, 125120 — Published 10 September 2018

DOI: 10.1103/PhysRevB.98.125120

Dyonic Lieb-Shultz-Mattis Theorem and Symmetry Protected Topological Phases in Decorated Dimer Models

Xu Yang,[1] Shenghan Jiang,[1] Ashvin Vishwanath,[2] and Ying Ran[1]

[1] *Department of Physics, Boston College, Chestnut Hill, MA 02467, USA*
[2] *Department of Physics, Harvard University, Cambridge, MA 02138, USA*

We consider 2+1D lattice models of interacting bosons or spins, with both magnetic flux and fractional spin in the unit cell. We propose and prove a modified Lieb-Shultz Mattis (LSM) theorem in this setting, which applies even when the spin in the enlarged magnetic unit cell is integral. There are two nontrivial outcomes for gapped ground states that preserve all symmetries. In the first case, exotic bulk excitations, i.e. topological order, is necessarily present even though the enlarged unit cell contains integer spin. In the second case, topological order can be avoided but then a symmetry protected topological (SPT) phase is necessarily realized. The resulting SPTs display a dyonic character in that they associate spin/charge with symmetry flux, allowing the flux in the unit cell to screen the fractional spin/charge on the sites. We provide an explicit formula that encapsulates this physics, which identifies a specific set of allowed SPT phases. This also provides a route to constructing models of SPT states by decorating dimer models of Mott insulators, which should be useful in their physical realization.

I. INTRODUCTION

The Lieb-Shultz-Mattis (LSM) theorem[1], appropriately generalized to higher dimensions[2–5], requires that a gapped spin system with fractional spin (eg. S=1/2) per unit cell possess excitations with fractional statistics (anyon) and fractional quantum numbers (topological order), if all symmetries (including lattice translations) are preserved. This has served as a powerful principle to diagnose exotic phases such as the fractional quantum Hall effect, and quantum spin liquids. Furthermore, in some cases the nature of the resulting topological order can be further constrained by the microscopic data[6,7].

In recent years there has been an explosion of activity on symmetry protected topological (SPT) phases, which feature protected boundary modes although the bulk is short range entangled (SRE) and in contrast to the situation above, is free of anyon excitations. These include phases like topological insulators, which can be captured by free fermion models[8,9], as well as intrinsically interacting phases[10–12] A natural question to ask is - are there setting where the microscopic data alone would enforce an SPT phase, in a fashion analogous to the LSM theorem? If so, for a particular set of microscopic data, can we further characterize precisely which kinds of SPT orders are mandated?

These questions are answered in the present work. We show that SPT order *must* arise when the following conditions are met. The first ingredient is magnetic translation symmetry, that is an enlargement of the unit cell due to the non-commutativity of the primitive translation operations. Second, we require that the primitive unit cell (ignoring the noncommutativity) does not admit a trivial insulating phase. This is arranged by requiring a projective representation at each lattice site. Finally, we need some compatibility conditions between these two ingredients that allow, among other conditions, that the enlarged unit cell to be effectively at integer filling, what admits a short range entangled ground state. The latter is then shown to be an SPT. Furthermore for 2+1D bosonic systems we explicitly calculate the allowed SPTs compatible with the microscopic specifications. In addition we construct exactly soluble lattice models of this phenomenon to demonstrate the validity of our conclusions. This general principle should aid in the search for SPTs in realistic settings and exposes anew aspect of the interplay between symmetry and topology.

To give some simple plausibility arguments as to how microscopic constraints can enforce SPT order, consider free fermions in a magnetic field, when the filling fraction (ratio of particle density to magnetic flux density) is an integer. Then, an integer number of Landau levels will be filled, leading to a Chern insulator - which is an SRE topological phase with gapless edge states. Even in the presence of a lattice , one can establish a similar connection between the Hall conductance σ_{xy}, the flux n_ϕ and electron filling in the unit cell n_e[13,14] which has been extended to the case of time reversal symmetric topological insulators[15].

To state our result more precisely, we consider a two dimensional lattice where the unit translations obey: $T_xT_yT_x^{-1}T_y^{-1} = g$, where g is an element of the symmetry group G. This generalizes the notion of a magnetic translation, particles acquire a phase factor depending on their g charge. We assume g is in the center of the symmetry group G (i.e. commutes with all other elements), but otherwise consider a general G, which can either be discrete or continuous, Abelian or nonAbelian, and can include time reversal implemented by an antiunitary representatation. Furthermore, in each unit cell a projective representation of the symmetry group labeled by 'α' is present. We derive a formula which provides a necessary and sufficient condition on these inputs to allow for an SRE phase, and determine constraints on the resulting SPT. Physically, this formula demands that a symmetry flux g inserted into this system will precisely generate a projective representation that can screen 'α'[15].

Let us give two physical pictures to view this filling and flux enforced SPTs. First we describe a vortex condensation based picture, for a system of lattice bosons with a conserved U(1) charge, with flux n_ϕ and filling n_b per lattice unit cell. Although our paper focuses on having projective representations per site (rather than fractional filling) this example will be useful to build intuition. It is well known that a conventional insulator can be thought of as a condensate of vortices. However, for fractional filling n_b, the vortices see a fractional flux per unit cell[16], and their condensate will break lattice symmetries. Similarly, the bosons themselves cannot condense without breaking lattice symmetries due to the fractional flux n_ϕ. *However* the bound state of a vortex and p bosons may be able to propagate freely if: $n_b \pm p n_\phi \in \mathcal{Z}$ is an integer. The resulting object is a boson for p even which can then condense giving rise to an SRE and symmetric insulator. These are nothing but the Bosonic Integer quantum Hall insulators at $\nu = n_b/n_\phi = p$[12,17,18]. Note, here the condensing particle carries unit vorticity and hence the resulting insulator is free of topological order[19] and also preserves the U(1) symmetry since the condensing charge is attached to vorticity. A generalization of this result to include arbitrary symmetry groups is the main result of this paper. An interesting exception occurs for $p = 1$, which is realized for example when one has bosons at half filling (or a projective representation of $U(1) \rtimes Z_2$), and a π flux in each unit cell. The doubled unit cell is at integer filling. At first sight it appears we can obtain an insulator by condensing the vortex-charge composite which sees no net flux in the unit cell. However, this composite is a fermion and cannot be condensed. This is also seen by a flux threading argument[14] that constrains such SRE phases to have σ_{xy} = odd integer, which is impossible for an SRE topological phase of bosons[17,18]. Interestingly, this result continues to hold if the $U(1)$ is broken to a discrete symmetry as shown below.

A second perspective is to begin in a topologically ordered phase with fractionalized excitations and consider confining all exotic excitations by an appropriate anyon condensate. For example, for bosons at half filling, one could obtain toric code (Z_2) topological order where the e particle carries half charge[20]. The m particle however sees the fractional charge density as background flux and cannot condense while preserving spatial symmetries. This is the situation in the absence of magnetic translations, where the LSM theorem enforces topological order for gapped symmetric states. However, once we allow for magnetic translations with g charge, a way out to an SRE phase may become available. The m particle, bound to a g charge that sees the magnetic flux, forms a composite object that may condense uniformly and confine the topological order. At the same time, this leads to an SPT phase since the condensing anyon carries nontrivial symmetry charge[21,22]. Indeed this picture will allows us to construct models of such LSM enforced SPT phases as we describe below.

Before discussing construction of models, it may be helpful to give a few examples. Consider a system of degenerate doublets ("S=1/2") on sites of a square lattice. This site degeneracy may arise from spin rotation invariance ($SO(3)$), or even just as Kramers degeneracy protected by time reversal Z_2^T symmetry. Now consider an additional Z_2 symmetry which is invoked in defining the magnetic translations, i.e. we have a fully frustrated Ising model on the same lattice. According to our results, in both these situations SRE ground states are possible but must be SPT phases. While the SPT phase is unique for the second case of Kramers doublets of $Z_T \times Z_2$, in the former case of $SO(3) \times Z_2$ there is more than one SPT phase possible. Interestingly, if we consider a minor modification of the $Z_T \times Z_2$ model, such that the doublets on each site are non Kramers pairs, protected by the combination of the two symmetries, then *no* SRE ground state exists (and hence no SPT exists) that respects all symmetries. These examples are discussed in detail in Section III A which also introduces models that realize them.

In constructing models, the first step is to begin in the deconfined phase of a discrete lattice gauge theory (or of a dimer model). Then, one way to obtain a confined phase is by decorating the electric field lines with domain walls of a global symmetry. This identification implies that we have condensed the composite of magnetic flux and symmetry charge. The resulting confined phase is potentially an SPT if the electric charges are associated with the appropriate symmetry fractionalization[21,22]. However, to obtain an LSM enforced SPTs the situation is different since they involve fractional spin on the sites. In a dimer model this corresponds to having an odd number of dimers associated with a unit cell, in which case we cannot decorate them with regular domain walls (which should be closed loops). *However* if the global symmetry is also associated with flux in the unit cell (for example a fully frustrated Ising model), the two kinds of frustration cancel each other out, and one can still achieve this decoration of electric field line. This is discussed explicitly in Section II, for a specific model and the resulting state is shown to be the desired SPT. The model there is one of hardcore bosons on the Kagome lattice tuned to half filling by particle hole symmetry, previously introduced by Balents, Fisher and Girvin[23]. While their focus was on a Z_2 spin liquid phase, we decorate their model with an additional Z_2 symmetry realized by a fully-frustrated Ising model. The combination is shown to realize an LSM enforced SPT phase with gapless edge states, but a short range entangled bulk.

Finally in SectionIII we discuss the problem for general symmetry groups, and derive the necessary and sufficient conditions for SRE phases to emerge and identify the class of SPTs that must be realized. Proofs are sketched in SectionV while the details can be found in the appendices.

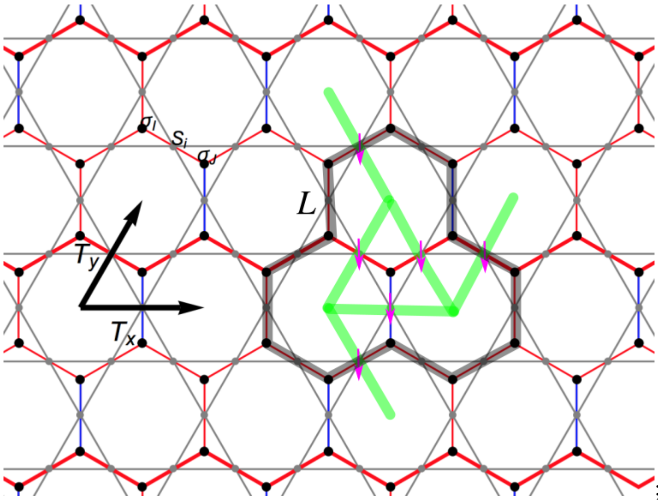

FIG. 1: (color online) Degrees of freedom in the decorated BFG model Eq.(1). The top-layer Ising d.o.f. σ_I ($\sigma_I^z = \pm 1$) live on the honeycomb lattice and the bottom-layer spin d.o.f. S_i ($S_i^z = \pm\frac{1}{2}$) lives on the Kagome lattice. The Ising coupling signs $s_{IJ} = +1$ on red bonds, and $s_{IJ} = -1$ on blue bonds. The thick red bonds represent the "y-odd zigzag chains" used in Eq. (18). A local area enclosed by the loop-L (thick gray loop) satisfying the low energy constraint (three spin-down per hexagon) is shown, together with the corresponding the electric field lines (thick green lines).

II. A SIMPLE MODEL REALIZING AN SPT PHASE

Our discussion starts from a concrete microscopic model realizing an SPT phase. The beauty of this model is its simplicity, which only includes two-spin and three-spin interactions. It turns out that the crucial features of this model can be systematically generalized which form the main results of the current study.

This model can be viewed as two coupled layers of spin-1/2 systems (see. Fig.1 for an illustration). The bottom layer is formed by an easy-axis XXZ spin model (Eq.2,5) living on the Kagome lattice proposed by Balents-Fisher-Girvin (BFG)[23], which only contains two-spin interactions and is known to realize an Z_2 spin liquid phase when decoupled from the top layer. The top layer is formed by a simple pure transverse field Ising model living on the honeycomb lattice (Eq.3) whose sites are sitting on top of the centers of the triangles in the Kagome bottom layer. This top Ising layer is in a trivial paramagetic phase if decoupled from the bottom layer (i.e., all Ising spins are polarized by the transverse field). We will use spin-S_i to label the d.o.f. in the bottom layer and spin-σ_I to label the d.o.f. in the top layer, where i, I label sites in the Kagome lattice and honeycomb lattice respectively.

Finally, the crucial ingredient of this model is the coupling between these two layers: Eq.(4). This coupling is formed by three-spin interactions. When the coupling constant is large, it is designed to confine the Z_2 gauge theory in the bottom layer without breaking physical symmetry, leading to an nontrivial SPT phase. As we will discuss shortly, one way to interpret this coupling is that it energetically decorates the electric field line in the Z_2 gauge theory in the bottom layer by the Ising domain wall in the top layer, and consequently confining the electric charge excitations. As another (equivalent) interpretation, this coupling is driving the Z_2 gauge fluxes (visons) in the bottom layer to condense, and the condensed visons carry the Ising charge of the top layer.

We now write down the full Hamiltonian of this model (see Fig.1):

$$H = H^{BFG} + H^{Ising} + H^{binding}, \tag{1}$$

where H^{BFG} is the BFG model living on the bottom Kagome layer, whose physics will be reviewed shortly:

$$\begin{aligned} H^{BFG} =& J_z \sum_{\hexagon} (\sum_{i\in\hexagon} S_i^z)^2 \\ &+ J_\perp \sum_{\hexagon} [(\sum_{i\in\hexagon} S_i^x)^2 + (\sum_{i\in\hexagon} S_i^y)^2 - 3], \end{aligned} \tag{2}$$

where the summations are over all hexagons in the Kagome lattice. H^{Ising} is the simple pure transverse field Ising model living on the top honeycomb layer:

$$H^{Ising} = h \sum_I \sigma_I^x, \tag{3}$$

and $H^{binding}$ is the coupling between the two layers, controlled by a coupling constant $\lambda > 0$:

$$H^{binding} = - \sum_{I \overset{i}{\bullet\!\!-\!\!\bullet} J} \lambda S_i^z \cdot (s_{IJ} \sigma_I^z \sigma_J^z). \tag{4}$$

Here the summation is over all the nearest neighbor bonds IJ on honeycomb lattice with S_i at the bond center. The sign $s_{IJ} = \pm 1$ are frustrated in the sense that $\prod_{I,J\in\hexagon} s_{IJ} = -1$, for every hexagon on the honeycomb lattice. We have specifically made a choice of s_{IJ} in Fig. 1. Basically, this coupling term energetically binds an Ising domain wall on the top layer ($\sigma_I^z \sigma_J^z = -1$) to the S^z-spin-down state in the bottom layer if $s_{IJ} = +1$, and to the S^z-spin-up state in the bottom layer if $s_{IJ} = -1$.

We firstly state our main result on this model. It is well-known that the BFG model H^{BFG} alone realizes a Z_2 spin liquid phase in the strong easy-axis regime $J_z \gg J_\perp$[23–25], with the deconfined Z_2 gauge charge excitation e carrying S^z spin-1/2. Such a state has been termed as a symmetry-enriched topological(SET) phase due to the presence of topological order as well as its interplay with global symmetries[26–29]. When the coupling strength $\lambda \to 0$, the ground state of the full model Eq.(1) is obviously a tensor product of the BFG Z_2 spin liquid state in the bottom layer and an Ising paramagnetic state (polarized by the transverse field) in the top layer. Our main claim here is that **in the parameter regime $J_z \gg \lambda \gg J_\perp, h$ and $\frac{h^2}{\lambda^2} \gg \frac{J_\perp}{J_z}$, the system can be shown in a nontrivial SPT phase.** Since the SPT phase has no topological order, the Z_2 gauge theory must be confined as λ is turned from 0 into the SPT regime. Such a schematic phase diagram is illustrated in Fig.2(a).

Preparing to justify our claim, we briefly review the basic features of the BFG model Eq.(2). In the strong easy-axis regime, $J_z \gg J_\perp$, the J_z term energetically enforces a constraint: for the six sites in every hexagon in the Kagome lattice, there are exactly three S^z-spin-up and three S^z-spin-down. All states satisfying this constraint form a low energy subspace. It is convenient to perform degenerate perturbation analysis of the $J_\perp$ term, leading to the following effective Hamiltonian:

$$H_{eff}^{BFG} = J_z \sum_{\hexagon} \Big(\sum_{i\in\hexagon} S_i^z\Big)^2$$

$$-J_{\text{ring}} \sum_{\bowtie} \Big(\Big|$$ 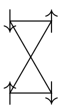 $$\Big\rangle\Big\langle$$ 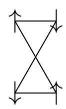 $$\Big| + h.c.\Big), \qquad (5)$$

with ring-exchange $J_{ring} = J_\perp^2/J_z$ around every bowtie. In the following our discussion will be based on H_{eff}^{BFG}.

Physically, one can interpret each S^z-spin-down (S^z-spin-up) as the presence (absence) of a Z_2 electric field line connecting two centers of the hexagons in the Kagome lattice (all such centers form a triangular lattice, see Fig.1). The low energy constraint means that there are exactly three electric field lines coming out of each triangular lattice site, as a Gauss' law. The J_{ring}-term generates fluctuations of the electric field lines, lifts the degeneracy of the low energy subspace leading to a Z_2 spin liquid ground state.

One can readily write down a loop operator detecting the Z_2 gauge charge enclosed by a contractable loop L formed by bonds on the honeycomb lattice (see Fig.1):

$$\hat{O}_L \equiv \prod_{k\in L} 2S_k^z. \qquad (6)$$

Note that $\hat{O}_L$ commutes with the effective Hamiltonian H_{eff}^{BFG}, and simply counts the parity of the electric field lines crossing L. In the low energy subspace, $\hat{O}_L$ has a fixed eigenvalue for a given L. When a Z_2 gauge charge excitation e is present inside L, the low energy constraint is violated and $\hat{O}_L$ changes sign.

On a torus, H_{eff}^{BFG} is known to feature four fold degenerate ground states in the thermodynamic limit. This can be understood by partitioning the Hilbert space into four topological sectors according to the parity of eigenvalues of $\hat{O}_L$ with L being non-contractable loops wrapping around the two holes of the torus. The local dynamics would only act within each topological sector.

A Z_2 gauge charge e carries half-integer S^z quantum number. One simple argument for this is that every nearest neighbor electric field line carries $S^z = -1$ (comparing a S^z-spin-down with a S^z-spin-up), which should be shared by the two end points of the electric field line. And e exactly corresponds to one such end point. More precisely speaking, one can define an operator measuring the local S^z-charge per hexagon:

$$S^z_{\hexagon} \equiv \sum_{k\in\hexagon} \frac{1}{2} S_k^z, \qquad (7)$$

where the factor $\frac{1}{2}$ is introduced since each S^z spin is shared by two neighboring hexagons. The total S^z-charge over a region D composed by many hexagons is simply:

$$S^z_D = \sum_{\hexagon\in D} S^z_{\hexagon}. \qquad (8)$$

We denote the boundary of D as ∂D. ∂D is a loop formed by bonds on the honeycomb lattice. For any site $i \in D$ and $i \notin \partial D$, $\frac{1}{2}S_i^z$ is summed twice and their total contribution to S_D^z is fixed modulo one for any $\{S_i^z\}$ configuration. To measure the half-integer S_i^z carried by a quasiparticle excitation inside D (relative to the ground state), one only need to consider the boundary contribution:

$$\big[S_D^z \mod 1\big] \sim \big[\sum_{k\in\partial D} \frac{1}{2} S_k^z \mod 1\big] \qquad (9)$$

Namely, if one flips a single S_k^z for $k \in \partial D$ (and therefore an electric line crossing ∂D is created/annihilated), $S_D^z \mod 1$ changes by 1/2. Now if $\hat{O}_L$ in Eq.(6) changes sign, there are two physical interpretations: first, an additional Z_2 gauge charge is created inside L; second, the S^z-charge inside L changes by a half-integer.

Since it is detecting the Z_2 gauge charge, $\hat{O}_L$ can be viewed as the braiding process of the Z_2 gauge flux (vison) around the loop L. Consequently one can define an open string operator creating a pair of visons by taking a open segment C connecting sites I and J on the honeycomb lattice:

$$v_I v_J \equiv \prod_{k\in C} 2S_k^z. \qquad (10)$$

When applying on the ground state, this operator creates a pair of visons at the I and J. In this Z_2 spin liquid phase, both the gauge charge and the vison are gapped topological excitations, with excitation energies $\sim J_z$ and $\sim J_{ring}$ respectively.

We are now ready to discuss the decorated full model Eq.(1). First, the full Hamiltonian can be separated into two parts $H = H_0 + H_1$:

$$\begin{aligned} H_0 &= J_z \sum_{\hexagon} (S^z_{\hexagon})^2 - \sum_{\substack{\mathrm{i} \\ \mathrm{I} \bullet\!\!-\!\!\bullet \mathrm{J}}} \lambda S_i^z (s_{IJ}\sigma_I^z \sigma_J^z). \\ H_1 &= J_\perp \sum_{\hexagon} [(S^x_{\hexagon})^2 + (S^y_{\hexagon})^2 - 3] + \sum_I h\sigma_I^x. \end{aligned} \qquad (11)$$

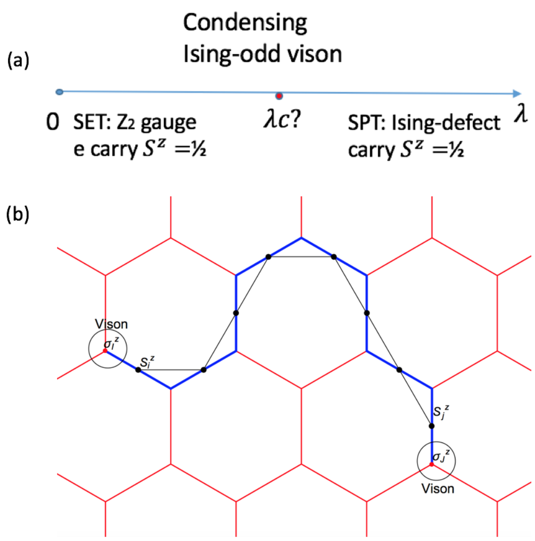

FIG. 2: (color online) (a) Schematic phase diagram of the decorated BFG model by tuning λ. We have already fixed $J_z \gg J_\perp, h$. In the limit $\lambda \to 0$ the Ising layer is decoupled and the ground state is just that of the original BFG model with Z_2 topological order. This is an SET state with spinon carrying $S^z = 1/2$. When λ is tuned to be within the parameter regime where $J_z \gg \lambda \gg J_\perp, h$ and $\frac{h^2}{\lambda^2} \gg \frac{J_\perp}{J_z}$, we have an SPT state with Ising defect carrying $S^z = 1/2$ as discussed in the main text. There is a possible direct phase transition triggered by the condensation of Ising-odd visons at some intermediate λ_c. (b) A schematic view of vison condensation. The honeycomb lattice where Ising d.o.f. lives is shown and the spin d.o.f. lives in the bond center. Two visons are created at the ends I, J of the string operator along C (blue string): $\sigma_I^z \sigma_J^z \prod_{k\in C} 2S_k^z$. with S_k^z runs over all the black dot shown in the graph. Alternatively we can view the string operator as the product of bond variable $S_i^z \sigma_H^z \sigma_K^z$ along C. Due to the constraint $2S_i^z(s_{HK}\sigma_H^z\sigma_K^z) = 1$, the string operator has a well-defined eigenvalue (product of s_{HK}'s along the blue bonds) acting in the low energy subspace, indicating that the visons are condensed and the Z_2 topological order is confined. Note that the condensed visons in the present case are dressed by local σ^z operator and hence carry the quantum number of the Ising symmetry, resulting in an SPT state.

H_0 contains terms that are mutually commuting. We will firstly analyze H_0 and treat H_1 as a perturbation.

H_0 gives a new low energy constraint: apart from the original constraint of three electric field line (S^z-spin-down) per hexagon in the bottom layer due to the J_z-term, the λ-term ($H^{binding}$) energetically binds each electric field line with an Ising domain wall in the top layer if and only if $s_{IJ} = 1$. Namely, we have new low energy constraints: $2S_i^z(s_{IJ}\sigma_I^z\sigma_J^z) = 1$ for every nearest neighbor $< IJ >$.

Because the low energy constraint $2S_i^z(s_{IK}\sigma_I^z\sigma_K^z) = 1$, the Ising domain wall configuration in the top layer is completely fixed for any given S^z-spin configuration $\{S_i^z\}$ in the bottom layer. Namely, for every $\{S_i^z\}$, there are two and only two quantum states in the low energy subspace, which we label as $|\{S_i^z, +\}\rangle$ and $|\{S_i^z, -\}\rangle$. They are related to each other by a global flip of the Ising spins: $|\{S_i^z, -\}\rangle = \prod \sigma_I^x |\{S_i^z, +\}\rangle$.

As a consequence of the new low energy constraint, the Z_2 gauge charge excitation e is confined. One way to see this is that when a pair of e is created and spatially separated by a distance l, the system would have an additional electric field open string connecting them. Along this electric field string, $2S_i^z(s_{IJ}\sigma_I^z\sigma_J^z) = 1$ constraints must be violated, leading to an energy cost $\propto l$ in $H^{binding}$, i.e., confinement.

The e confinement also signals the condensation of the visons. Indeed one can write down an vison-pair creation operator for the decorated model:

$$v_I^{deco.} v_J^{deco.} \equiv \sigma_I^z \sigma_J^z \prod_{k\in C} 2S_k^z. \tag{12}$$

The only difference from the original vison-pair creation operator Eq.(10) is the two local operators σ_I^z, σ_J^z at the two ends of C. Due to the $2S_i^z(s_{HK}\sigma_H^z\sigma_K^z) = 1$ low energy constraints, $v_I^{deco.} v_J^{deco.}$ has a fixed eigenvalue in the decorated low energy subspace (product of s_{HK} along C), i.e., vison condensation. In addition, the additional σ^z operators at the end of the string indicate that the condensed visons carry the Ising symmetry σ^x charge. See Fig.2(b) for an illustration. In fact, according to Ref.[21], starting from the Z_2 spin liquid phase with e charge carrying half-integer-S^z, the Ising-odd vison condensation necessarily gives rise to a nontrivial SPT phase.

We have established the Ising domain wall decoration and the new low energy subspace. Now we introduce H_1 as a perturbation. In particular, we consider the perturbative regime: $J_z \gg \lambda \gg J_\perp, h$ and $\frac{h^2}{\lambda^2} \gg \frac{J_\perp}{J_z}$. Degenerate perturbation analysis leads to the following effective Hamiltonian: (see Appendix. A for detailed calculations)

$$H_{eff}^{deco.BFG} = H_0$$

$$- \frac{10 J_\perp^2 h^2}{9 J_z \lambda^2} \sum_{\bowtie} (| \quad \rangle\langle \quad | + h.c.). \tag{13}$$

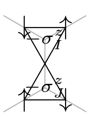

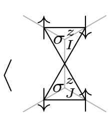

The kinetic terms (the second line) in this effective Hamiltonian are ring exchange terms of four spins in each bowtie as in H_{eff}^{BFG}, but combined with the flipping the two Ising spins inside the bowtie such that the constraint $2S_i^z(s_{IJ}\sigma_I^z\sigma_J^z) = 1$ is perserved.

Our discussion below will be based on $H_{eff}^{deco.BFG}$. We shall prove that it has a unique ground state on the torus, which is a nontrivial SPT state. In fact, the energy spectrum in the Ising-even low energy sector of $H_{eff}^{deco.BFG}$

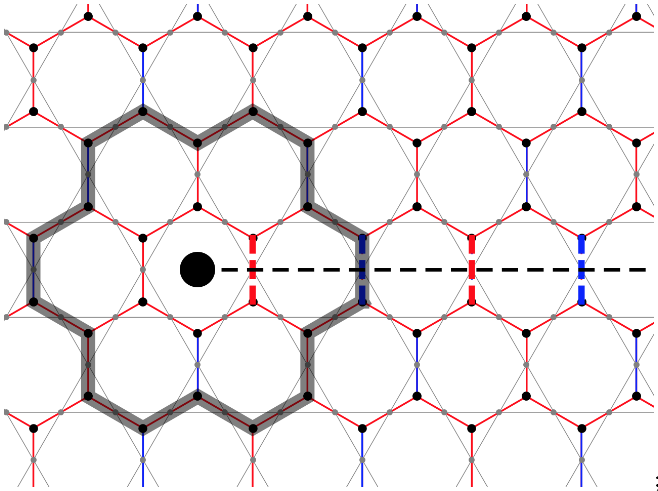

FIG. 3: (color online) An pair of Ising defects (only one is shown) is created at the end points of the branch cut (dashed black line) after modifying the original Hamiltonian H in Eq.(1) into H'. The sign s_{IJ} is flipped in H' along the branch cut comparing with the original model. (red bond: $s_{IJ}=+1$, blue bond: $s_{IJ}=-1$) For any loop-L enclosing the Ising symmetry defect as the gray loop shown here, the product $\prod s_{IJ}$ around the loop flips sign comparing with the original model. Due to the low energy constraint $2S^z_i(s_{IJ}\sigma^z_I\sigma^z_J)=1$, the total S^z around the loop-L is changed by an odd integer comparing to the case without an Ising defect. The result is that Ising defect is topologically bound with a half-integer spin. See the discussion in the main text.

can be immediately obtained from that of H^{BFG}_{eff} using an isometry mapping $\mathcal{P}$ between the two low energy sub-Hilbert spaces:

$$\mathcal{P}:(|\{S^z_i,+\}\rangle+|\{S^z_i,-\}\rangle)/\sqrt{2}\rightarrow|\{S^z_i\}\rangle, \tag{14}$$

we have

$$\mathcal{P}H^{deco.BFG}\mathcal{P}^{-1}=H^{BFG}, \tag{15}$$

with the identification $J_{ring}=\frac{10J_\perp^2h^2}{9J_z\lambda^2}$, which can be proven by directly comparing the matrix elements on the two sides.

Note that the isometry $\mathcal{P}$ can be viewed as a unitary mapping from the Ising-even low energy sector of $H^{deco.BFG}_{eff}$ onto a specific topological sector of H^{BFG}_{eff} on a torus: due to the constraint $2S^z_i(s_{IJ}\sigma^z_I\sigma^z_J)=1$, $\prod(2S^z_i)$ around any loop is fixed by s_{IJ}. Because H^{BFG}_{eff} is completely gapped inside a specific topological sector, $H^{deco.BFG}_{eff}$ is also gapped in the Ising-even sector. The ground state $|\psi^{deco.}\rangle$ in the Ising-even sector of $H^{deco.BFG}_{eff}$, should also be mapped to a ground state $|\psi\rangle$ of H^{BFG}_{eff}. However there is still one possibility that there exists low energy state in the Ising-odd sector which becomes degenerate with $|\psi^{deco.}\rangle$ – a hallmark of the Ising symmetry breaking.

This possibility is ruled out because $|\psi^{deco.}\rangle$ has no long-range Ising order. One can explicitly compute the Ising correlator in $|\psi^{deco.}\rangle$. After choosing a open string C with ends points being σ_I and σ_J, based on the discussion below Eq.(12):

$$\begin{aligned}|\langle\psi^{deco.}|\,\sigma^z_I\sigma^z_J\,|\psi^{deco.}\rangle\,|&=|\,\langle\psi^{deco.}|\prod_{k\in C}2S^z_k\,|\psi^{deco.}\rangle\,|,\\&=|\,\langle\psi|\prod_{k\in C}2S^z_k\,|\psi\rangle\,|,\end{aligned} \tag{16}$$

where the last correlator exhibits exponential decay since visons are deconfined and gapped in the original effective BFG model H^{BFG}_{eff} (the last equality holds because $\mathcal{P}$ commutes with the string operator).

In fact, based on the well-known duality between the Ising model and the Z_2 gauge theory[30], one can further show that the spectrum of the Ising-odd sector of $H^{deco.BFG}_{eff}$ is above the energy of $|\psi^{deco.}\rangle$ by a finite energy gap. This can be done as follows. The spectrum in the Ising-odd sector of $H^{deco.BFG}_{eff}$ can be mapped via a unitary transformation $U=\sigma^z_I$ (where this I is an arbitrarily chosen site) to the Ising-even sector of the modified Hamiltonian $H^{deco.BFG}_{mod}=UH^{deco.BFG}_{eff}U^{-1}$. Then under the isometry $\mathcal{P}$, we have

$$\mathcal{P}H^{deco.BFG}_{mod}\mathcal{P}^{-1}=H^{BFG}_{mod}. \tag{17}$$

Simple algebra shows that H^{BFG}_{mod} is the same as H^{BFG}_{eff} except that the ring-exchange terms of the three bowties enclosing site I are changed in sign. As discussed in Ref.24, the ground state of this Hamiltonian is just a single vison state. This is reasonable from the Ising-gauge duality since σ^z_I in the Ising model side is identified as vison creation operator in the gauge theory side.

The ground state energy of H^{BFG}_{mod} is larger than the ground state energy of H^{BFG}_{eff} by an amount identified as the vison energy gap[24]. Since the unitary transformation U and the isometry $\mathcal{P}$ both preserve the energy spectrum, we know immediately that the Ising-odd sector of $H^{deco.BFG}_{eff}$ has an energy gap from the ground state $|\psi^{deco.}\rangle$, whose size is identical to the vison energy gap in H^{BFG}_{eff}. This completes our proof that the ground state of $H^{deco.BFG}_{eff}$ is $|\psi^{deco.}\rangle$, which is a symmetric SRE state.

Finally we show that the ground state $|\psi^{deco.}\rangle$ is a nontrivial SPT state by considering the Ising symmetry defect, which turn out to be topologically bound with a half-integer S_z-charge – a projective representation of the symmetry group (see discussion below). By definition, in order to introduce a pair of Ising defects one takes an open branch cut and modify the local Hamiltonian terms straddling it, such that only the Ising spins on one side of the branch cut are conjugated by the Ising symmetry $\prod\sigma^x_I$. The net effect is that for the any nearest neighbor bond $< IJ >$ crossing the branch cut, the sign of s_{IJ} is flipped. See Fig. 3 for an illustration.

Due to the low energy constraint $2S_i^z(s_{IJ}\sigma_I^z\sigma_J^z) = 1$, one can immediately observe that $\prod_{i\in L} 2S_i^z$ flip sign for any loop-L enclosing one end of the branch cut (i.e., the Ising symmetry defect). Based on the discussion below Eq.(9), the Ising defect carries a half-integer S_z.

Summary: Before proceeding let us pay close attention to the symmetry property of the Hamiltonian in Eq. (1). This model has the following $Z_{2g} \times (U(1) \rtimes Z_{2h})$ onsite symmetry

1. Spin-rotation symmetry $U(1)$: $\prod_i e^{i\theta(S_i^z + \frac{1}{2})}$, with $\theta \in [0, 2\pi)$.

2. Spin-flip and Ising-flip symmetry $Z_{2h} = \{I, h\}$: $\prod_i S_i^x \prod_{I\in A} \sigma_I^x$, which flips all the spins on Kagome lattice and Ising d.o.f on the A-sublattice of the honeycomb lattice. This symmetry operation leaves the Hamiltonian in Eq. (1) invariant.

3. Ising symmetry $Z_{2g} = \{I, g\}$: $\prod_I \sigma_I^x$, which flips all the Ising d.o.f. on the honeycomb lattice.

The onsite symmetry group has the direct product structure $G = Z_{2g} \times (U(1) \rtimes Z_{2h})$. In addition, every unit cell (three kagome sites and two honeycomb sites) carries a nontrivial projective representation of $U(1) \rtimes Z_{2h}$ (i.e. a half-integer spin). If the system respects the usual translation symmetries the (generalized) LSM theorem would rule out a symmetric short-range-entangled ground state. However, the Ising-couplings in the binding terms $H^{binding}$ are fully frustrated. The system actually respects magnetic translation symmetries T_x, T_y instead of usual translations $T_x^{orig.}, T_y^{orig.}$:

$$\begin{aligned} T_x &= (\prod_{I\in \text{y-odd zigzag chains}} \sigma_I^x) T_x^{orig.}, \\ T_y &= T_y^{orig.}, \end{aligned} \tag{18}$$

which satisfy the magnetic translation algebra

$$T_x T_y T_x^{-1} T_y^{-1} = g. \tag{19}$$

It turns out that the system has a unique symmetric ground state realizing a non-trivial SPT phase, respecting all the onsite symmetries and the magnetic translation symmetries. We also showed that the g-defect (Ising symmetry defect) carries an half-integer S^z, which is the same projective representation carried by every unit-cell. Below we will show that this is not a coincidence and can be systematically generalized. In fact, in the presence of the onsite symmetries and magnetic translation symmetries, it is often true that the only possible symmetric short-range entangled ground states are non-trivial SPT phases: a phenomenon we term as "symmetry-enforced SPT phases".

III. MAIN RESULTS

Our main results are captured in two theorems. Theorem-I is easier to state but less general. Theorem-II is more general but is more mathematically involved to state.

Consider a two-dimensional *bosonic* quantum system respecting an onsite symmetry group G (which could contain time-reversal), and g is a unitary symmetry element in the center of G (i.e., g commutes with any element in G). The system respects a "magnetic" translation symmetry group generated by T_x, T_y satisfying the algebra:

$$T_x T_y T_x^{-1} T_y^{-1} = g, \tag{20}$$

where T_x, T_y are assumed to be the usual translation operations combined with certain site-dependent onsite unitary transformations. We further assume that the physical degrees of freedom (d.o.f.) in each real space unit cell (*not* the enlarged magnetic unit cell) form a nontrivial projective representation α of G, specified by a 2-cocycle: $\forall a, b \in G, \alpha(a, b) \in U(1)$ and $\alpha \in H^2(G, U(1))$. Precisely, the unitary or antiunitary transformation U_a, U_b of $a, b \in G$ satisfy:

$$U_a {}^a U_b = \alpha(a, b) U_{ab}, \tag{21}$$

where the left-superscript a in ${}^aU_b$ denotes the group action of a on U_b: if a is unitary (antiunitary), then ${}^aU_b = U_b$ (${}^aU_b = U_b^*$, i.e. complex conjugation of U_b).

We ask the following question: is it possible for such a system to have a short-range entangled(SRE) gapped ground state without breaking symmetries?

Here we use the definition of SRE states following Ref. 12; i.e., those are gapped quantum phases that can be deformed into the trivial product state via local unitary transformations. Note that if the system respects usual translational symmetries, this would be impossible: constrained by a generalized Lieb-Schultz-Mattis theorem[1,2,4], the nontrivial projective representation per unit cell indicates that a gapped liquid ground state necessarily features topological order. Here because the system respects a magnetic translation symmetry, it is possible that an SRE liquid ground state exists. We give sufficient and necessary conditions for such a liquid phase to exist, and show that this SRE liquid phase must be an SPT phase.

In the presence of an onsite symmetry group G, focusing on bosonic systems specified by Eq.(20,21), we have the following theorems:

Theorem-I: Here we further assume that $G = G_1 \times Z_N$ where Z_N is the finite abelian subgroup generated by g. The quantum system above can have an SRE liquid ground state if and only if the two conditions below are both satisfied. Such a liquid phase is necessarily a nontrivial SPT phase because the g-symmetry defect must carry the projective representation α.

1. $\alpha^N \simeq \mathbf{1} \in H^2(G, U(1))$, i.e. N of these projective representations fuse into a regular representation.

2. The group function (which maps elements of the symmetry group to phases, while preserving the group relations) $\gamma_g^\alpha(a) \equiv \frac{\alpha(g,a)}{\alpha(a,g)}, \forall a \in G$ is a trivial 1-cocycle (or equivalently, a trivial one-dimensional representation):
$\gamma_g^\alpha \simeq \mathbf{1} \in H^1(G, U(1))$.

What is the physical meaning of these two conditions? The first condition is well anticipated, which ensures that the enlarged magnetic unit cell does not have projective representations. If the first condition is not satisfied, the generalized Lieb-Schultz-Mattis theorem[1,2,4] already forbids an SRE liquid phase when applying on the magnetic unit cell. Interestingly, this is not sufficient to ensure an SRE phase. Additionally, condition 2 must be satisfied, which essentially states that the symmetry involved in magnetic translations, g, can be chosen to commute with all other projective group actions in a proper gauge. In the next section we will present examples in which condition 2 plays important role.

When these conditions are satisfied we can explicitly identify the 3-cocycle of at least one allowed SPT phase as follows. Note, given the direct product structure of the symmetry group, every element $a \in G$ can be associated with a corresponding element in Z_N, labeled n_a. Then, the 3-cocycle characterizing one allowed SPT is:

$$\omega(a, b, c) = [\alpha(b, c)]^{-n_a s_a}, \tag{22}$$

where $s_a = +1$ or -1 depending on whether a is unitary or antiunitary, and we have chosen a canonical gauge for α so that $\alpha(b, c)^N = 1, \forall b, c$ and $\alpha(g, b) = \alpha(b, g), \forall b \in G$. (see Appendix B for details.)

Theorem-II: Here we do not make extra assumptions on G. The quantum system above can have an SRE liquid ground state if and only if there exists a 3-cocyle ω_0: $\forall a, b, c \in G, \omega_0(a, b, c) \in U(1)$ and $\omega_0 \in H^3(G, U(1))$, such that the group function $\delta_g^{\omega_0}(a, b) \equiv \frac{\omega_0(g,a,b)\omega_0(a,b,g)}{\omega_0(a,g,b)}$ is 2-cycle equivalent to α^{-1}: $\delta_g^{\omega_0} \simeq \alpha^{-1} \in H^2(G, U(1))$. If such a quantum system has an SRE ground state, it is necessarily a nontrivial SPT phase because the g-symmetry defect must carry the projective representation α. The possible nontrivial SPT phases form a coset from the classification point of view (see Remark below).

Remark: it is straightforward to show that $\forall \alpha \in H^2(G, U(1))$, $\gamma_g^\alpha \in H^1(G, U(1))$. And similarly $\forall \omega \in H^3(G, U(1))$, $\delta_g^\omega \in H^2(G, U(1))$. The mappings $\gamma_g : H^2(G, U(1)) \to H^1(G, U(1))$ and $\delta_g : H^3(G, U(1)) \to H^2(G, U(1))$ reducing a n-cocycle to a $(n-1)$-cocycle are the so-called slant-products in mathematical context. γ_g and δ_g preserve the multiplication relation in the cohomology group. In particular, there is a subgroup $\mathcal{A}_g \in H^3(G, U(1))$ such that $\forall \omega \in \mathcal{A}_g, \delta_g^\omega \simeq \mathbf{1} \in H^2(G, U(1))$, (i.e., $\mathcal{A}_g$ the kernel of the mapping δ_g).

When the condition in Theorem-II is satisfied, ω_0 must be a nontrivial element in $H^3(G, U(1))$ because α is nontrivial by assumption. And the realizable SPT phases form a coset from the classification point of view. More precisely, the 3-cocycle characterizing the SRE liquid phase must be one of the element in the following coset: $\omega_0 \cdot \mathcal{A}_g$.

Outline of the proof: The proof of these theorems is a combination of a pumping argument of entanglement spectra and derivations/constructions based on a recently developed symmetric tensor-network formulation[21], which we outline here. Basically, if an SRE liquid phase exists, by the pumping argument of entanglement spectra one knows that *the g-symmetry-defect in this phase must carry the projective representation α, and consequently this phase must be an SPT phase*. This physical observation can be further justified by calculations based on symmetric tensor-networks, leading to the following mathematical result: if the 3-cocycle characterizing the SRE liquid phase as $\omega \in H^3(G, U(1))$, then magnetic translation symmetry dictates $\delta_g^\omega \simeq \alpha^{-1}$, which is exactly the same mathematical condition for the g-symmetry-defect carrying the projective representation α. In addition, based on the symmetric tensor-network formulation, for any ω satisfying $\delta_g^\omega \simeq \alpha^{-1}$, an SRE liquid phase characterized by ω respecting the magnetic translation symmetry can be constructed. These prove that the conditions in Theorem-II are *necessary and sufficient* for the SRE liquid phase to exist. In addition, when ω_0 exists, because a 3-cocycle $\omega \in H^3(G, U(1))$ satisfies $\delta_g^\omega \simeq \alpha^{-1}$ if and only if $\omega \in \omega_0 \cdot \mathcal{A}_g$, the coset structure in the Remark is also established.

Theorem-I is just a special case of Theorem-II. Namely when $G = G_1 \times Z_N$, one can show that if and only if the two conditions in Theorem-I is satisfied does the condition in Theorem-II is satisfied. The condition-(2) is less obvious and more interesting, which puts additional constraints for the existence of an SRE liquid phase (see example-(4) below).

Before going into the details of the proof, we present a few simple examples to see the applications of the Theorems and the Remark.

A. Examples

In these examples, the element g in the magnetic translation algebra Eq.(20) generates a $Z_2^{Ising} \equiv \{I, g\}$ Ising symmetry group. For instance, a fully frustrated

Ising model on the square lattice would satisfy this magnetic translation symmetry. The symmetry-enforced SPT phases in example-(1,2) will be demonstrated via a class of decorated quantum dimer models, which are exactly solvable at the Rokhsar-Kivelson points[31].

(1) $\mathbf{G = SO(3) \times Z_2^{Ising}}$, and a spin-1/2 per unit cell: Namely, the projective representation α per unit cell is nontrivial because only the $SO(3)$ part is projectively represented, and the Ising and the spin-rotation still commute: $\alpha(g,a) = \alpha(a,g)$, $\forall a \in G$. Clearly the two conditions in Theorem-I are both satisfied. First, two spin-1/2's fuse into a regular $SO(3)$ representation, and $\gamma_g^\alpha(a) = 1, \forall a \in G$.

According to Theorem-I, at least one SRE liquid phase can exist and must be an SPT phase in which the g-symmetry-defect carries a half-integer spin. To understand how many SPT phases are possibly realized, one can follow the Remark.[32] The result is that among all possible SPT phases classified by $H^3(SO(3) \times Z_2^{Ising}, U(1)) = Z \times Z_2^2$, only one of the Z_2 indices is enforced to be nontrivial. And there are many distinct SPT phases that can be realized, which form a coset $\omega_0 \cdot \mathcal{A}_g$, where $\mathcal{A}_g = Z \times Z_2$. *In particular, after gauging the Z_2^{Ising} symmetry, one may obtain either the toric-code or double-semion topological order, depending on which SPT phase is realized.*

(2) $\mathbf{G = Z_2^T \times Z_2^{Ising}}$, and a Kramer doublet per unit cell: Here $Z_2^T = \{I, \mathcal{T}\}$ is the time-reversal symmetry group. Denoting the Ising and time-reversal transformations on the physical d.o.f. in one unit cell as U_g, and $U_\mathcal{T}$ (antiunitary), the projective representation α per unit cell satisfies:

$$U_g^2 = 1, \qquad U_\mathcal{T} U_\mathcal{T}^* = -1, \qquad U_\mathcal{T} U_g^* = U_g U_\mathcal{T}. \tag{23}$$

For instance, this algebra is satisfied if $U_g = \sigma_x$ and $U_\mathcal{T} = i\tau_y$ for a four-dimensional local Hilbert space (upon which σ and τ Pauli matrices act). One can check that the two conditions in Theorem-(1) are both satisfied, and thus *at least an SRE liquid phase can exist and must be an SPT phase in which the g-symmetry-defect carries the projective representation α (a Kramer-doublet) above.*

Naively this example is very similar to the example-(1). However there is an important difference. In this example, *only one SPT phase can be realized* — following the Remark, this is because the kernel subgroup $\mathcal{A}_g$ is the trivial Z_1 group.[33] *After gauging the Z_2^{Ising} symmetry, one must obtain a toric code topological order.* This realizable SPT phase is topologically identical to the one obtained by decorating Ising domain walls with the Z_2^T Haldane chains[34].

(3) $\mathbf{G = Z_2' \times Z_2^{Ising}}$, and a projective representation per unit cell: In this example, $Z_2' = \{I, h\}$ is another unitary Ising symmetry group. The projective representation α satisfies:

$$U_g^2 = 1, \qquad U_h^2 = 1, \qquad U_g U_h = -U_h U_g. \tag{24}$$

For instance, $U_g = \sigma_x$, $U_h = \sigma_z$ realize this algebra. Two of such projective representations fuse into a regular representation of G, so the condition-(1) in Theorem-(1) is satisfied. But one can show that the condition-(2) is *not* satisfied:

$$\gamma_g^\alpha(h) = -1, \tag{25}$$

i.e., γ_g^α is a nontrivial 1-cocycle. Therefore according to Theorem-(1), *an SRE liquid phase is not possible.* Without breaking symmetry, this suggests that topological order is inevitable for gapped systems. This is a somewhat surprising result. If one views the system using the enlarged magnetic unit cell, there is no reason why an SRE liquid is not allowed.

IV. DECORATED QUANTUM DIMER MODELS FOR SPT PHASES

Closely related to the decorated-BFG model in Sec.II, in this section we describe a class of exactly solvable models realizing symmetry-enforced SPT phases. These models are constructed by decorating quantum dimer models(QDM) with relevant physical degrees of freedom, whose ground states can be exactly solved at the corresponding Rokhsar-Kivelson point[31]. Although this class of models can be generalized to other lattices, here we will focus on the decoration of the QDM on the triangular lattice[35,36]. In particular, we will construct models realizing the symmetry-enforced SPT phases in example-(1,2) in Sec.III A.

A. $G = SO(3) \times Z_2^{Ising}$, a spin-1/2 per unit cell

Continuing with discussions in example-(1) in Sec.III A, in the presence of onsite global symmetry $G = SO(3) \times Z_2^{Ising}$, we consider quantum systems with one spin-1/2 per unit cell in two spatial dimensions respecting the Ising magnetic translation symmetry Eq.(20). Note that we will reserve symbols T_x, T_y for the magnetic translations, and use $T_x^{orig.}, T_y^{orig.}$ to represent the original translations.

We will construct two exactly solvable models (model-A and model-B) respecting the symmetry described above featuring SRE liquid ground states. Although the Ising defects in both models carry half-integer spins, the two models are in distinct SPT phases. The simplest way to understand their difference is that, after gauging the Ising symmetry, model-A has toric-code topological order while model-B has double-semion topological order.

We start with constructing model-A. This model contains two sets of degrees of freedom (d.o.f.): the Ising-d.o.f. σ_I which live on a honeycomb lattice and the spin-1/2-d.o.f. $\mathbf{S}_i = \boldsymbol{\tau}_i/2$ which live on the triangular lattice formed by centers of the hexagons, as shown in Fig.4. The Hamiltonian of model-A contains three terms:

$$H = H^{Ising} + H^{binding} + H^A. \tag{26}$$

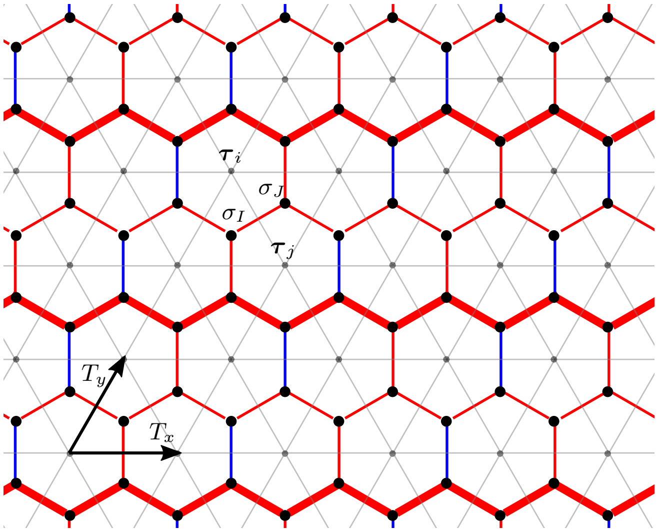

FIG. 4: (color online) The Ising d.o.f. σ live on the honeycomb lattice and the spin d.o.f. $\boldsymbol{\tau}$ lives on the triangular lattice. The Ising coupling signs $s_{IJ} = +1$ on red bonds, and $s_{IJ} = -1$ on blue vertical bonds. The thick red bonds represent the "y-odd zigzag chains" used in Eq.(29).

where H^{Ising} is simply a frustrated nearest-neighbor Ising model:

$$H^{Ising} = -K \sum_{\langle IJ \rangle} s_{IJ} \sigma_I^z \sigma_J^z. \tag{27}$$

Here σ_I^z, σ_J^z are the Ising spins living on the honeycomb sites labled by I, J, the coupling constant $K > 0$, and $s_{IJ} = \pm 1$ defined as in Fig.4. $H^{binding}$ is an interaction between the Ising-d.o.f. and spin-1/2-d.o.f., which commutes with H^{Ising}:

$$H^{binding} = -\lambda \sum_{\substack{\mathrm{J} \\ \mathrm{i} \,+\, \mathrm{j} \\ \mathrm{I}}} \frac{1}{2}(1 - s_{IJ}\sigma_I^z \sigma_J^z) \cdot \hat{P}_{\mathbf{S}_i + \mathbf{S}_j = 0}, \tag{28}$$

where $\lambda > 0$, i, j labels the sites on the triangular lattice, and the summation of "$+$" is over all intersection points between the triangular lattice and the honeycomb lattice as shown in Fig.4. $\hat{P}_{\mathbf{S}_i + \mathbf{S}_j = 0} \equiv \frac{1}{4} - \mathbf{S}_i \cdot \mathbf{S}_j$ is the operator projecting the two spin-1/2's on site-i and site-j into a spin singlet.

H^A is more complicated and will be given in Eq.(33). It is straightforward to checked that H respects the Ising symmetry $U_g \equiv \prod_I \sigma_I^x$, the spin-rotation symmetry generated by $\sum_i \mathbf{S}_i$. H also respects magnetic translation operations:

$$T_x = \Big(\prod_{I \in \text{y-odd zigzag chains}} \sigma_I^x\Big) \cdot T_x^{orig.}, \quad T_y = T_y^{orig.}, \tag{29}$$

(see Fig.4), and the magnetic translation algebra Eq.(20) is satisfied. We will show that the ground state of H is in a gapped liquid phase without topological order. According to our general results, this ground state must be in an SPT phase, which we will show momentarily.

The physical consequence of H^{Ising} and $H^{binding}$ is to provide a highly degenerate low energy manifold, which will be lifted by H^A. To understand the low energy manifold, let us firstly consider H^{Ising}. Because every hexagonal plaquette frustrated, there will be at least one bond in each plaquette that is energetically unhappy. Namely the ground state manifold of H^{Ising} is formed by all possible Ising configurations satisfying the "one-unhappy-Ising-bond-per-plaquette" condition.

$H^{binding}$ further constrains the spin-1/2 d.o.f. in the low energy manifold. It has effect only on the Ising unhappy bonds ($s_{IJ}\sigma_I^z\sigma_J^z = -1$), and energetically binds the two spin-1/2's near the unhappy Ising-bond into a spin singlet. The degenerate ground state manifold of $H^{Ising} + H^{binding}$ is now clear: it is formed by all such quantum states satisfying the "one-unhappy-Ising-bond-per-plaquette" condition and the two neighboring spin-1/2's normal to every unhappy Ising-bond form a spin singlet.

It is well-known that the Ising configurations satisfying the "one-unhappy-Ising-bond-per-plaquette" condition are intimately related to the Hilbert space of the QDM[37–39]. Pictorially, any such an Ising configuration can be mapped to a dimer covering (with one dimer per site) on the triangular lattice by assigning a dimer crossing the unhappy Ising bond. The effect of $H^{binding}$ is simply to energetically binds the two spin-1/2's in each dimer into a spin-singlet. Namely if the Ising configuration is given, the state of spin-1/2 d.o.f. is also fixed after choosing a sign convention for the spin singlets. For instance, we choose a translationally symmetric sign convention for the spin-singlets on the nearest neighbor bonds along the three orientations:

$$
\begin{aligned}
|\,\text{—}\,\rangle &\equiv \frac{1}{\sqrt{2}}\big(|\uparrow\!-\!\downarrow\rangle - |\downarrow\!-\!\uparrow\rangle\big),\\
|\,\diagdown\,\rangle &\equiv \frac{1}{\sqrt{2}}\big(|\,{\downarrow}\!\diagdown\!{\uparrow}\,\rangle - |\,{\uparrow}\!\diagdown\!{\downarrow}\,\rangle\big),\\
|\,\diagup\,\rangle &\equiv \frac{1}{\sqrt{2}}\big(|\,{\downarrow}\!\diagup\!{\uparrow}\,\rangle - |\,{\uparrow}\!\diagup\!{\downarrow}\,\rangle)\big\rangle.
\end{aligned} \tag{30}
$$

Similar to the model in Sec.II, we are decorating the electric field line (i.e., the dimer) with the "one-unhappy-Ising-bond-per-plaquette" of the Ising d.o.f., and there is an isometry mapping $\mathcal{P}$ from the Ising-even sector of the ground state manifold of $H^{Ising} + H^{binding}$ to the QDM Hilbert space. Any dimer covering $|c\rangle$ corresponds to two Ising configurations $|c_+\rangle$ and $|c_-\rangle$ in the ground state manifold of $H^{Ising} + H^{binding}$, related to each other by a global Ising flip. $\mathcal{P}$ sends $(|c_+\rangle + |c_-\rangle)/\sqrt{2}$ to $|c\rangle$, and $\mathcal{P}$ only maps onto one specific topological sector of the QDM: The parity of the number of dimers crossing a loop is simply given by the sign of the product $\prod_{\langle IJ \rangle \in loop} s_{IJ}$.

After introducing H^A, we will see that the degeneracy in the low energy manifold is lifted and the unique ground state on a torus sample is formed. The usual QDM Hamiltonian on the triangular lattice is:

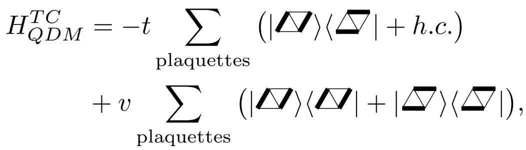

(31)

where the summation is over all plaquettes (rhombi): . The ground states of this model are exactly known at the RK-point given by $t = v > 0$, and the superscript TC is highlighting that the topological order is toric-code[35,40] like in the deconfined phase (i.e., the usual Z_2 gauge theory). At this point H^{TC}_{RK} can be rewritten as a summation of projectors[35]:

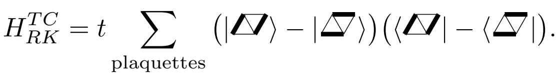

(32)

Clearly the equal weight superposition of all dimer coverings within any fixed topological sector $|\Phi^{TC}_{RK}\rangle = \sum_c |c\rangle$ (c labels possible dimer coverings) is one ground state of H^{TC}_{RK} since it is annihilated by all projectors.

We will design H^A such that the isometry mapping sends H^A to H^{TC}_{QDM}:

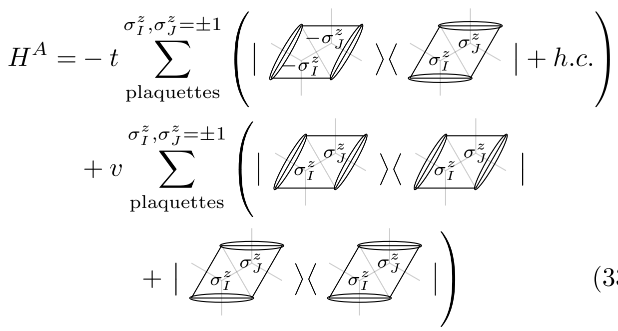

(33)

Note that the t-term also flips the two Ising spins inside the plaquette. At the RK point $t = v > 0$, H^A can again be written as a summation of projectors:

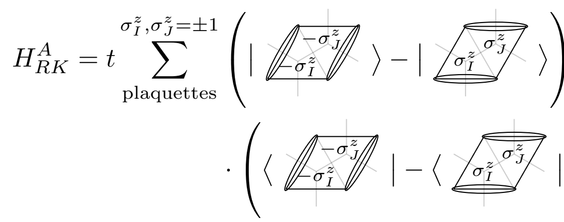

(34)

To study the ground state of the total Hamiltonian H, it is suffice to focus on the degenerate ground state manifold of $H^{Ising} + H^{binding}$, and clearly H^A acts within this manifold. In addition, it is straightforward to show that $|\Phi^A_{RK}\rangle = \sum_c (|c_+\rangle + |c_-\rangle)$, i.e, the equal weight superposition of all states in this manifold, is a ground state of H^A_{RK} because it is annihilated by every projector in Eq.(34). $|\Phi^A_{RK}\rangle$ is clearly a fully symmetric liquid wavefunction.

It is known that for the QDM Eq.(31), the RK point of H is exactly at a first-order phase transition boundary between a deconfined gapped liquid phase ($v < t$) and a staggered valence bond solid phase ($v > t$)[35]. Similar to the discussion in Sec.II, the model-A is in a fully symmetric gapped liquid phase for $v_c < v < t$ with a unique ground state on torus. In the limit of $K, \lambda \gg v, t$, v_c is given by the same critical value $v_c \approx 0.7t$ as in the original QDM[35].

Next we show that the liquid phase $v_c < v < t$ in model-A is an SPT phase because the Ising defects carry half-integer spins. Similar to the discussion in Sec.II (see Fig.3), after a pair of Ising defects are spatially separated the original Hamiltonian H is modified into H'. Comparing with H, the s_{IJ} flips sign in H' whenever the bond $I - J$ crosses the branch cut. Namely, for any loop on the honeycomb lattice enclosing a single Ising defect, the product $\prod s_{IJ}$ along the loop changes sign. In order not to cost $H'^{binding}$ energy, the parity of the number of dimers crossing this loop also flips. Consequently, an Ising defect is topologically bound with a monomer (an unpaired site on the triangular lattice). And this monomer clearly carries a half-integer spin in model-A.

Next, we demonstrate a different symmetry-enforced SPT phase using the model-B defined as follows:

$$H = H^{Ising} + H^{binding} + H^B. \tag{35}$$

Comparing with the model-A in Eq.(26), only the last term is modified:

$$H^B = v \sum_{\text{plaquettes}}^{\sigma_I^z,\sigma_J^z=\pm1} \Big(|\ \sigma_I^z\ \sigma_J^z\ \rangle\langle\ \sigma_I^z\ \sigma_J^z\ | + |\ \sigma_I^z\ \sigma_J^z\ \rangle\langle\ \sigma_I^z\ \sigma_J^z\ | \Big) + \sum^{\sigma_I^z,\sigma_J^z=\pm1} \Big(-it|\ -\sigma_I^z\ -\sigma_J^z\ \rangle\langle\ \sigma_I^z\ \sigma_J^z\ | + h.c. \Big)$$
$$+ \sum^{\sigma_I^z,\sigma_J^z=\pm1} \Big(-it|\ -\sigma_J^z\ -\sigma_I^z\ \rangle\langle\ \sigma_J^z\ \sigma_I^z\ | + h.c. \Big) + \sum^{\sigma_I^z,\sigma_J^z=\pm1} \Big(-it|\ -\sigma_I^z\ -\sigma_J^z\ \rangle\langle\ \sigma_I^z\ \sigma_J^z\ | + h.c. \Big) \tag{36}$$

One can straightforwardly check that the model-B defined in Eq.(35,36) also respects the Ising symmetry, the $SO(3)$ spin-rotation symmetry, and the magnetic translation symmetry Eq.(20). Below we show that in a finite parameter regime $v_c' < v < t$, the model-B is in a gapped liquid phase, and this phase is another SPT phase.

In the ground state manifold of $H^{Ising} + H^{binding}$, the duality transformation maps H^B into the following QDM Hamiltonian:

$$H_{QDM}^{DS} = v \sum_{\text{plaquettes}} \big(|\ \rangle\langle\ | + |\ \rangle\langle\ | \big)$$
$$+ \sum -it\big(|\ \rangle\langle\ | + |\ \rangle\langle\ | + |\ \rangle\langle\ | \big) + h.c. \tag{37}$$

This QDM was firstly introduced and studied in Ref. 36, where the exactly solvable RK point $t = v$ has been shown to be adjacent a gapped liquid phase for $v \lesssim t$. Interestingly, this phase was demonstrated to have a double-semion topological order (the superscript DS here is to highlight this fact). By the isometry mapping, we know that in a finite parameter regime $v_c' < v < t$, the model-B is in a gapped liquid phase.

Similar to previous discussion on the model-A, it is straightforward to show that the Ising defect in the gapped liquid phase of model-B also carries half-integer spin, so it is also an SPT phase. To see the difference from the SPT phase realized in model-A, let us consider the Ising symmetry only. It is known that Ising symmetry itself can protect two paramagnetic phases: the trivial phase and the SPT phase. Levin and Gu pointed out[41] that the duality mapping maps the usual Ising paramagnet to the toric-code topological order, while the nontrivial Ising SPT phase maps to the double semion topological order. Our decoration of the electric-field line with Ising-unhappy-bond is exactly such a duality mapping. Consequently, the SPT phases realized in model-A and model-B are different because the Ising symmetry alone already distinguishes them.

B. $G = Z_2^T \times Z_2^{Ising}$

Here we demonstrate symmetry-enforced SPT phases outlined in example-(2) in Sec.III A. Unlike the $G = SO(3) \times Z_2^{Ising}$ case, here we show that symmetry conditions fully determine the SPT phase. The models below have the same Hilbert space as in the $G = SO(3) \times Z_2^{Ising}$ case (i.e., σ_I on the honeycomb lattice and $\boldsymbol{\tau}_i$ on the triangular lattice), but with different symmetries defined.

A Kramer doublet per unit cell: A simple generalization is for example-(2) (i.e., a Kramer-doublet per unit cell) where we can recycle the model-A. Namely, defining the Ising symmetry $U_g = \prod_I \sigma_I^x$ as before and the anti-unitary time-reversal symmetry as $e^{i\pi \mathbf{S}^y} \cdot K$ (K is the complex conjugation), clearly model-A respect all the these onsite symmetries together with the same magnetic translation symmetry Eq.(29). In addition, we have one Kramer doublet $\boldsymbol{\tau}$ per unit cell. According to our discussion in example-(2), this SRE liquid phase realized in $v_c < v < t$ must be an SPT phase in which the Ising defect carries a Kramer doublet, which is obviously realized in model-A. In addition, after gauging Z_2^{Ising} symmetry, one necessarily obtains the toric-code topological order, which is confirmed in model-A.

On the other hand, model-B, gauging which gives double-semion topological order, explicitly breaks the time-reversal symmetry defined above.

V. PROOF OF THEOREMS

Here we present a combination of physical argument and mathematical derivations based on symmetric tensor network formulation[21,42–49]. We will focus on Theorem-II, and in AppendixB we show that Theorem-I can be viewed as its special case.

We need to show the condition in Theorem-II is necessary and sufficient for an SRE liquid phase to exist, which must be an SPT phase. To show this condition is necessary, we consider such an SRE liquid phase and the pumping of the entanglement spectra during an adiabatic process in Sec.V A, leading to an observation that a g-symmetry defect must carry a projective representation α. In an SRE liquid phase characterized by 3-cocycle ω, we use the symmetric tensor-network formulation in Sec.V B to establish that the projective representation carried by a g-symmetry defect is given by $(\delta_g^\omega)^{-1}$. Together we show that the SRE liquid must satisfy $(\delta_g^\omega)^{-1} = \alpha$, i.e., this condition is necessary.

As a complementary calculation, we also explicitly

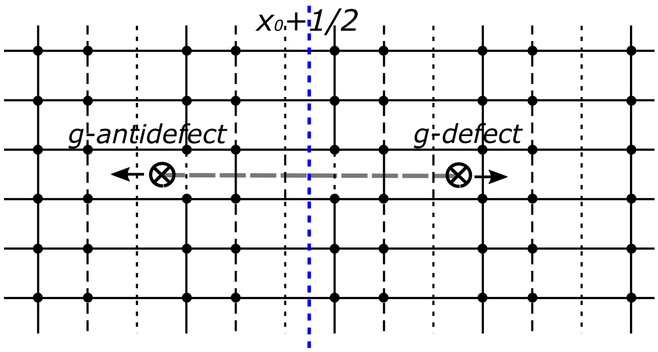

FIG. 5: Illustration of adiabatically separating a pair of g-defect/antidefect along the x-direction with $g^3 = I$. For simplicity, one may imagine Hamiltonian to host nearest neighbor (NN) terms. Along the x-direction, due to the magnetic translation symmetry Eq.(20), the NN interactions on the vertical bonds have a three-unit-cell periodicity (solid,dashed and dotted bonds). While the g-defect crosses the entanglement cut at $x_0 + 1/2$, the Hamiltonian along the branch cut (dashed gray line) is effectively translated along x-direction by one unit cell. After separating such pairs of defects for every row, the final Hamiltonian is related to the original Hamiltonian by $T_x^{orig.}$.

compute the projective representation carried by a g-symmetry defect in an SRE liquid phase representable within the symmetry tensor-network formulation in Appendix.E, which turns out to be α, consistent with the previous discussion[50].

To further show that the condition is also sufficient, we will show that for any 3-cocycle ω_0 satisfying $(\delta_g^{\omega_0})^{-1} \simeq \alpha$, generic symmetric tensor network wavefunctions representing an SRE liquid phase characterized by ω_0 can be constructed in Sec.V C.

A. Entanglement Pumping argument

Here let us assume an SRE liquid phase exist. It is straightforward to show that after a local unitary transformation, one can always choose a gauge in which $T_y = T_y^{orig.}$ and $T_x = (\prod_{y-odd} U_g) \cdot T_x^{orig.}$. Then we consider putting this SRE liquid on a infinite cylinder C along the x-direction, with L_y number of unit cells across the y-direction loop. We choose $L_y = l_y \cdot N + d_y$ where l_y, d_y are integers, $g^N = I$ and $0 \leq d_y < N$. Note that if $d_y \neq 0$ this choice of L_y will explicitly break the T_x symmetry.

This infinite long cylinder can be viewed as a one-dimensional system, and for a large enough L_y the onsite symmetry G will be respected. We will study the entanglement spectrum of this one dimensional system at a particular cut $x_0 + 1/2$. An SRE liquid respecting G symmetry dictates that entanglement states at this cut carry a particular projective representation ξ of G[51,52].

Next, we adiabatically create a g-symmetry defect/anti-defect pair at a given y-coordinate and separate them to infinity along the x-direction. After repeating this procedure for every y-coordinate, we totally move L_y number of g-symmetry defects across the entanglement cut $x_0 + 1/2$. As shown in Fig.5, the final Hamiltonian is related with the original Hamiltonian by the *original* translation operation $T_x^{orig.}$. Therefore, the final entanglement states at the cut $x_0 + 1/2$ is equivalent to the initial entanglement states at a different cut: $x_0 - 1/2$.

Because the initial entanglement states at $x_0 - 1/2$ differs from the initial entanglement states at $x_0 + 1/2$ by a column of unit cells along y-direction, we conclude that the final entanglement eigenstates at $x_0 + 1/2$ must carry the $\alpha^{d_y} \cdot \xi$ projective representation. This pumping of the entanglement projective representation can only be explained by the projective representation $\tilde{\alpha}$ carried by a g-symmetry defect, and $(\tilde{\alpha})^{L_y} \simeq \alpha^{d_y}$. But because N g-defect fuse into a trivial object, we must have $(\tilde{\alpha})^N \simeq 1$. Consequently $\tilde{\alpha} = \alpha$.

B. Symmetry-enforced constraints on SPT cocycles

Here we consider an SPT wavefunction represented using the symmetric tensor-network formulation[21]. The advantage of this formulation is that it allows us to introduce symmetry defects conveniently.

The local symmetry transformation of an onsite symmetry a on a g-defect is given by the application of of U_a inside a disk D covering the g-defect, together with an application of unitary operations on the virtual degrees of freedom on the boundary of D. This boundary operation should be defined in such a way that after these two operations, no excitation is created near the boundary of D. In Appendix D we explicitly construct such boundary operations. With these boundary operations, we explicitly show that the projective representaion carried by the g-defect is given by $(\delta_g^{\omega})^{-1}$ in an SPT phase characterized by the 3-cocycle ω, which is given without proof in Ref. 50.

C. Generic constructions of Symmetry-enforced SPT wavefunctions

Our strategy here is to start from an SPT state characterized by a 3-cocycle ω with a regular representation of G per unit cell and respecting the usual translation symmetry $T_x^{orig.}, T_y^{orig.}$. Such a state can be generically represented using the symmetric tensor-network formulation[21]. In particular, the symmetric tensor-network needs to satisfy a collection of algebraic equations (constraints). Then we show that after properly modifying these algebraic constraints, the new tensor-network will respect the magnetic translation symmetry T_x, T_y. At the same time the physical d.o.f. must carry a projective representation $(\delta_g^\omega)^{-1}$ per unit cell (otherwise the wavefunction vanishes). The tensor-network states satisfying these modified constraints are generic constructions of the SPT states in Theorem-II.

The details of the construction can be found in Appendix F.

VI. DISCUSSION

Generalized Hastings-Oshikawa-Lieb-Schultz-Mattis theorems put strong constraints on possible symmetric quantum states of matter. In particular, in the presence of translation symmetry and a projective representation of the onsite symmetry group per unit cell, it is impossible to have a gapped short-range entangled (SRE) symmetric ground state. In this paper we discuss that in the presence of magnetic translation symmetry, gapped SRE symmetric ground states could exist, which are enforced to be symmetry protected topological (SPT) phases. Focusing on bosonic systems in two spatial dimensions, we provide the generic necessary and sufficient condition for such symmetry-enforced SPT phases to occur in Theorem-I and II. When the condition is satisfied, we sharply characterize the coset structure of the realizable SPT phases in the Remark.

The condition-(2) in Theorem-I is particularly nonobvious. It states that if symmetries protecting the fractional spin (projective representation) per unit cell and those generating the magnetic translations fail to commute with one another, then SRE liquid state is impossible even if the fractional spins fuse into an integer spin (regular representation) in the magnetic unit cell.

In addition, we design a class of decorated quantum dimer models realizing some of these symmetry-enforced SPT phases, which are exactly solvable at the corresponding Rokhsar-Kivelson points. A particularly simple model realizing a symmetry-enforced SPT phase is given in Sec.II by coupling a Balents-Fisher-Girvin spin liquid with a layer of pure-transverse-field Ising spins via three-spin interactions. This model also demonstrates the route to obtain SPT phases via condensing anyons in SET phases[21,22].

Recently, generalizations of LSM theorems to spin systems on non-symmorphic lattices have appeared[53,54], which bears some resemblance to the current problem, and it would be interesting to investigate if deeper connections exist. It is also interesting to consider the situation of fermions with magnetic translation symmetries, in which case (generalized) Hastings-Oshikawa-Lieb-Schultz-Mattis theorem apply for fractional filled systems with regular translation symmetries. In fact, earlier works[13,14] establish the magnetic translation symmetry protected integer Hall conductivity, and a recent work by Wu et.al. studied the magnetic translation enforced quantum spin Hall insulators in fractionally filled fermionic systems[15]. A very recent work by Lu also studies a class of SPT phases with magnetic translation symmetry enforced by LSM-type theorems for various bosonic and fermionic systems.[55] Connecting with these works, the present work focuses on bosonic systems with projective representation per unit cell, but obtains systematic results.

YR would like to thank Yuan-Ming Lu and Masaki Oshikawa for inspiring related collaborations[14]. XY, SJ and YR are supported by NSF under Grant No. DMR-1151440. AV is funded by a Simons Investigator award.

Appendix A: Perturbation study of the decorated Balents-Fisher-Girvin model

The Hamiltonian for the decorated BFG model can be split into two parts

$$
\begin{aligned}
&H^{deco.BFG} = H_0 + H_1, \\
&H_0 = J_z \sum_{\hexagon} (S^z_{\hexagon})^2 - \sum_{\substack{\mathrm{i} \\ \mathrm{I}\ \bullet\!-\!\bullet\ \mathrm{J}}} \lambda S^z_i (s_{IJ}\sigma^z_I \sigma^z_J), \\
&H_1 = J_\perp \sum_{(i,j)} S^+_i S^-_j + \sum_I h\sigma^x_I,
\end{aligned}
\tag{A1}
$$

where (i,j) runs over first, second, third neighbors within a hexagon of Kagome plaquette.

Let's take the limit $J_z, \lambda \gg J_\perp, h$ and only focus on the low energy Hamiltonian in the ground state manifold of H_0. Then we can treat H_1 as a small perturbation and use the conventional Brillouin-Wigner perturbation to derive the effective Hamiltonian. The effective Hamiltonian is then given by (take E_0 as the ground state energy of H_0),

$$
H_{eff} = E_0 + P_g(H_1 + H_1 G'_0 H_1 + H_1 G'_0 H_1 G'_0 H_1 + \cdots)P_g,
\tag{A2}
$$

where $G'_0 = P_e(E_0 - H_0)^{-1} P_e$ and P_g/P_e are the projector onto the ground/excited states of H_0.

We will work under the limit $J_z \gg \lambda$ and calculate the effective Hamiltonian order by order to find the leading non-constant terms in $J_\perp$ and h since we have not specified the relation between them yet. Let's denote N as the number of Kagome unit-cell. The zeroth order energy is $E_0 = -\frac{3}{2}N\lambda$. Higher order terms are as follows:

1. $H_{eff}^{(1)} = P_g H_1 P_g = 0$.

2. $H_{eff}^{(2)} = P_g H_1 G_0' H_1 P_g = -9N\frac{J_\perp^2}{2J_z+2\lambda} - 2N\cdot\frac{h^2}{3\lambda}$. The first term comes from the process of switching a pair of spin-up and spin-down and then switching back within a hexagon. The second term comes from the process of flipping a Ising d.o.f. twice. To this order, we only have constant terms.

3. $H_{eff}^{(3)} = P_g H_1 G_0' H_1 G_0' H_1 P_g = \frac{J_\perp^3}{(2J_z+2\lambda)^2}\sum_{(i,j,k)}(S_i^+S_k^-S_k^+S_j^-S_j^+S_i^- + S_j^+S_k^-S_i^+S_j^-S_k^+S_i^-)$, where the summation runs over all ordered triplets (i,j,k) with $(i,j),(j,k),(k,i)$ appearing in H_1. The term $S_i^+S_k^-S_k^+S_j^-S_j^+S_i^- = (1/2+S_i^z)(1/2-S_j^z)(1/2-S_k^z)$ measures the energy of the configuration with $S_i^z = 1/2, S_j^z = -1/2, S_k^z = -1/2$. And the term $S_j^+S_k^-S_i^+S_j^-S_k^+S_i^- = (1/2+S_i^z)(1/2+S_j^z)(1/2-S_k^z)$ measures the energy of the configuration with $S_i^z = 1/2, S_j^z = 1/2, S_k^z = -1/2$. To this order, the term does depend on the spin configuration and is the leading non-constant term in $J_\perp$.

4. $H_{eff}^{(4)} = P_g H_1 G_0' H_1 G_0' H_1 G_0' H_1 P_g = -\frac{10J_\perp^2h^2}{9J_z\lambda^2}\sum_{\bowtie}(|$ 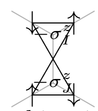 $\rangle\langle$ 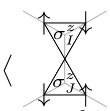 $| + h.c.) + \mathcal{O}(\frac{h^4}{\lambda^3}) + \mathcal{O}(\frac{J_\perp^2h^2}{J_z\lambda^2}) + \mathcal{O}(\frac{J_\perp^4}{J_z^3})$, where we have used the limit $J_z \gg \lambda$. The first term is a kinetic term which is the leading non-constant contribution in h. The latter three terms are not written out explicitly due to the following reason. Terms proportional to $\frac{J_\perp^4}{J_z^3}$ are less significant compared to that from the 3-rd order perturbation. Terms proportional to $\frac{h^4}{\lambda^3}$ (process of flipping two different Ising d.o.f. twice) is a constant. And the potential term proportional to $\frac{J_\perp^2h^2}{J_z\lambda^2}$ (process of separately flipping Ising d.o.f twice and exchanging spin-up and down twice) is also a constant in the limit $J_z \gg \lambda$.

The leading non-constant terms are terms of order $\frac{J_\perp^3}{J_z^2}$ and terms of order $\frac{J_\perp^2h^2}{J_z\lambda^2}$, where the latter is what we want. So we further require $\frac{h^2}{\lambda^2} \gg \frac{J_\perp}{J_z}$ such that the term obtained from the 3rd-order perturbation can be neglected.

Then we achieve the decorated BFG model

$H_{eff} = -\frac{10J_\perp^2h^2}{9J_z\lambda^2}\sum_{\bowtie}(|$ 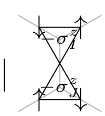 $\rangle\langle$ 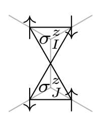 $| + h.c.)$ (A3)

in the parameter regime where $J_z \gg \lambda \gg J_\perp, h$ and $\frac{h^2}{\lambda^2} \gg \frac{J_\perp}{J_z}$.

Appendix B: Theorem-I as a special case of Theorem-II

1. Necessary condition for the existence of SRE states: constraints on the on-site projective representation

First we prove that only when the on-site projective representation α satisfies the following 2 conditions is an SRE ground state possible.

1. $\alpha^N \simeq \mathbf{1} \in H^2(G, U(1))$.
2. $\gamma_g^\alpha(a) \simeq \mathbf{1} \in H^1(G, U(1))$.

Suppose the unit-cell is enlarged along x-direction to include N original unit-cell, then we have $T_x^N T_y T_x^{-N} T_y^{-1} = g^N = \mathbf{1}$, *i.e.*, we have usual translation T_x^N, T_y in the enlarged unit-cell. From Hastings' theorem we know that for an SRE ground state to exist, the enlarged unit-cell must carry usual representation. Hence we know α^N is a trivial 2-cocycle.

Next, we know from Theorem-II that for such an SRE state to exist, there must exist a 3-cocycle $\omega \in H^3(G, U(1))$, such that $\delta_g^\omega(a,b) = \alpha(a,b)^{-1}$ up to a 2-coboundary. By tuning the 2-coboundary of $\alpha(a,b)$, we are tuning the 1-coboundary of $\gamma_g^\alpha(a)$. Therefore we have $\gamma_g^\alpha(a) \simeq \gamma_g^\omega(a)$, where $\gamma_g^\omega(a) \equiv \frac{\delta_g^\omega(a,g)}{\delta_g^\omega(g,a)}$.

$$\begin{aligned} \delta_g^\omega(a,g) &= \frac{\omega(a,g,g)\omega(g,a,g)}{\omega(a,g,g)} = \omega(g,a,g), \\ \delta_g^\omega(g,a) &= \frac{\omega(g,a,g)\omega(g,g,a)}{\omega(g,g,a)} = \omega(g,a,g). \end{aligned} \tag{B1}$$

Therefore we always have $\gamma_g^\omega(a) = 1$, which means $\gamma_g^\alpha(a) \simeq \mathbf{1} \in H^1(G, U(1))$.

2. Sufficient condition for the existence of SRE state: explicit construction of the 3-cocycle

We shall show that the necessary condition given in the last section is also sufficient. To be more specific, we will construct a 3-cocycle $\omega \in H^3(G, U(1))$ out of α given $\alpha^N \simeq \mathbf{1} \in H^2(G, U(1))$ and $\gamma_g^\alpha(a) \simeq \mathbf{1} \in H^1(G, U(1))$, such that $\delta_g^\omega(a,b) = \alpha(a,b)^{-1}$. From Theorem-II, we know that such an SRE state described by 3-cocycle $\omega \in$

$H^3(G, U(1))$ always exist, which completes our proof of Theorem-I.

a. Canonical gauge choice for $\alpha(a,b)$

Let's first fix a canonical gauge of $\alpha(a,b)$. Due to the direct product structure $G = G_1 \times Z_N$, we denote a general group element $a \in G$ as

$$a = g^{n_a} h_a, n_a = 0, 1 \cdots N-1, h_a \in G_1. \tag{B2}$$

We are given the condition that α^N is a trivial 2-cocycle in $H^2(G, U(1))$. Let's first tune the 2-coboundary of $\alpha(a,b)$ such that $\alpha^N = 1$. Then $\alpha(a,b) \in Z_N$.

We also know that

$$\gamma_g^\alpha(a) \in B^1(G, U(1)). \tag{B3}$$

If G_1 is a unitary group, then $\gamma_g^\alpha(a) \equiv 1$. If G_1 has anti-unitary operations, we should generally represent $\gamma_g^\alpha(a)$ as the 1-coboundary $\frac{\gamma}{^a\gamma}$.

Therefore we know that

$$\frac{\alpha(g,a)}{\alpha(a,g)} = \frac{\gamma}{^a\gamma} \in Z_N, \to \gamma \in Z_{2N}. \tag{B4}$$

We choose the 2-coboundary $\delta(a) = \delta(g)^{n_a}$ where $\delta(g) = \gamma^{N-1}$.

Then under the 2-coboundary $\delta(a)$ we have

$$\alpha(a,b) \to \frac{\delta(g)^{n_a} \cdot^a (\delta(g)^{n_b})}{\delta(g)^{\langle n_a + n_b \rangle_N}} \alpha(a,b), \tag{B5}$$

where $\langle n \rangle_N = n$ for $n < N$ and $\langle n \rangle_N = n - N$ for $n \geq N$.

Here the change of $\alpha(a,b)$ is always a Z_N element since

$$\begin{aligned}
&\frac{\delta(g)^{n_a} \cdot^a (\delta(g)^{n_b})}{\delta(g)^{\langle n_a + n_b \rangle_N}} \\
&= \begin{cases} (\frac{^a\gamma}{\gamma})^{(N-1)n_b} \in Z_N, \text{if } n_a + n_b < N. \\ (\frac{^a\gamma}{\gamma})^{(N-1)n_b} \cdot \gamma^{N(N-1)} \in Z_N, \text{if } n_a + n_b \geq N. \end{cases}
\end{aligned} \tag{B6}$$

Then after the change of 2-coboundary, we still have $\alpha^N = 1$.

But $\gamma_g^\alpha(a)$ is changed as follows

$$\gamma_g^\alpha(a) = \frac{\alpha(g,a)}{\alpha(a,g)} \to \frac{\delta(g)}{^a\delta(g)} \cdot \frac{\gamma}{^a\gamma} = \frac{\gamma^N}{^a\gamma^N} = 1, \tag{B7}$$

where we have used Eq. (B6) and the fact that $\gamma^{2N} = 1$. Then after the change of 2-coboundary we always have $\gamma_g^\alpha(a) = 1$.

In summary, we have fixed $\alpha^N = 1$ and $\alpha(g,a) = \alpha(a,g)$ as the canonical gauge choice.

b. Explicit construction of 3-cocycle

With the condition $\alpha^N = 1$ and $\alpha(g,a) = \alpha(a,g)$, we can explicitly construct the 3-cocycle as follows:

$$\omega(a,b,c) = [\alpha(b,c)^{-1}]^{n_a s_a}, s_a = 1/{-1} \text{ for } a \text{ unitary/anti-unitary}. \tag{B8}$$

First let's prove $\omega(a,b,c)$ is indeed a 3-cocycle. We have

$$\begin{aligned}
&\omega(a,b,c)\omega(a,bc,d)\omega(b,c,d)^{s_a} \\
&= [\alpha(b,c)^{-1}]^{n_a s_a} [\alpha(bc,d)^{-1}]^{n_a s_a} [\alpha(c,d)^{-1}]^{n_b s_a s_b} \\
&= [\alpha(c,d)^{-1}]^{n_a s_a s_b} [\alpha(b,cd)^{-1}]^{n_a s_a} [\alpha(c,d)^{-1}]^{n_b s_a s_b},
\end{aligned} \tag{B9}$$

where in the last equality we have used the 2-cocycle condition of α, *i.e.*,

$$\alpha(b,c)\alpha(bc,d) = \alpha(c,d)^{s_b} \alpha(b,cd). \tag{B10}$$

And we also have

$$\begin{aligned}
&\omega(ab,c,d)\omega(a,b,cd) \\
&= [\alpha(c,d)^{-1}]^{(\langle n_a + n_b \rangle_N) s_a s_b} \cdot [\alpha(b,cd)^{-1}]^{n_a s_a},
\end{aligned} \tag{B11}$$

which equals Eq. (B9) since $\alpha^N = 1$. Therefore ω satisfies the 3-cocycle condition

$$\omega(a,b,c)\omega(a,bc,d)\omega(b,c,d)^{s_a} = \omega(ab,c,d)\omega(a,b,cd). \tag{B12}$$

Next we show that the slant product of ω with respect to g gives us α^{-1},

$$\begin{aligned}
\delta_g^\omega(a,b) &= \frac{\omega(a,b,g)\omega(g,a,b)}{\omega(a,g,b)} = \frac{[\alpha(b,g)^{-1}]^{n_a s_a} [\alpha(a,b)^{-1}]}{[\alpha(g,b)^{-1}]^{n_a s_a}} \\
&= \alpha(a,b)^{-1},
\end{aligned} \tag{B13}$$

where we have used $\alpha(b,g) = \alpha(g,b)$.

Appendix C: A brief introduction to symmetric tensor network representation of SPT phases

In this appendix we want to briefly summarize the symmetric tensor network representation of SPT phases and fix the notations for future convenience. More details of the general formalism can be found in Ref. 21 and 49.

1. Basic set-up

Let's consider a PEPS state formed by infinite numbers of site tensors and discuss the symmetry implementation on such state[42–49]. We assume that for a symmetric PEPS the symmetry transformed tensors and the original tensors are related by a gauge transformation:

$$W_g g \circ \mathbb{T} = \mathbb{T}, \tag{C1}$$

where $\mathbb{T}$ is the tensor states with all internal legs uncontracted and W_g is the product of the gauge transformation acting on all internal legs of the tensor network.

The invariant gauge group (IGG) is the group of all the gauge transformations leaving the uncontracted tensor $\mathbb{T}$ invariant. These are denoted as global IGG in contrast to the plaquette IGG introduced later. The global IGG naturally arises from the following tensor equations:

$$\mathbb{T} = W_a a W_b b \circ \mathbb{T} = W_{ab} ab \circ \mathbb{T}, \tag{C2}$$

from which we know that

$$W_a \cdot^a W_b = \eta(a,b) W_{ab}, \tag{C3}$$

where $\eta(a,b)$ should leave the tensor invariant and hence is an IGG element.

And we have the associativity condition for $\eta(a,b)$:

$$\eta(a,b)\eta(ab,c) =^{W_a a} \eta(b,c)\eta(a,bc). \tag{C4}$$

The global IGG elements are a characteristic of symmetry breaking or topological order. In order to obtain an SPT state, we require all the global IGG elements can be decomposed into the product of plaquette IGG elements as shown in Fig 6, *i.e.*, $\eta(a,b) = \prod_p \lambda_p(a,b)$. There is a global phase ambiguity in such decomposition, namely we have $\prod_p \lambda_p = \prod_p \chi_p \lambda_p$ with χ_p a global phase since $\prod_p \chi_p = I$. The decomposible global IGG tells us that topological order is killed and the resulting phases should be an SPT phase described by the 3-cocycle ω, which arises as the phase ambiguity when lift Eq. (C4) to plaquette IGG,

$$\lambda_p(a,b)\lambda_p(ab,c) = \omega_p(a,b,c)^{W_a a}\lambda_p(b,c)\lambda_p(a,bc). \tag{C5}$$

The ω shown above is a well-defined 3-cocycle since the phase ambiguities in λ will only modify it by a 3-coboundary.

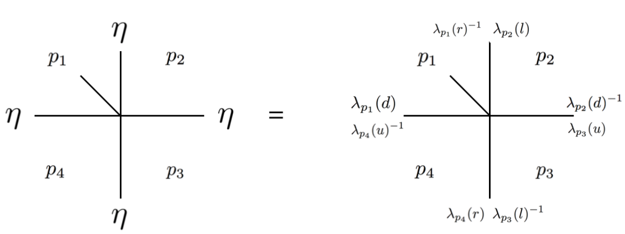

FIG. 6: The decomposition of global IGG into plaquette IGG. λ's from different plaquettes commutes with each other, and the action of any two λ's in the same plaquette leave the tensor invariant.

2. Representation of $\delta_g^\omega(a,b)$ using plaquette IGG

In this subsection we want to give a representation of the slant product $\delta_g^\omega(a,b)$ in terms of plaquette IGG for an SPT state characterized by 3-cocycle ω, where g lies in the center of the whole symmetry group G. First, from definition we have

$$\delta_g^\omega(a,b) = \frac{\omega(a,b,g)\omega(g,a,b)}{\omega(a,g,b)} \tag{C6}$$

The 3-cocycle arises from the decomposition of global IGG into the plaquette IGG, see Eq. (C5). Therefore in order to compute $\delta_g^\omega(a,b)$, we need the following equations:

$$\begin{aligned}
\lambda_p(a,b)\cdot\lambda_p(ab,g) &= \omega(a,b,g)\cdot^a \lambda_p(b,g)\cdot\lambda_p(a,bg),\\
\lambda_p(g,a)\cdot\lambda_p(ga,b) &= \omega(g,a,b)\cdot^g \lambda_p(a,b)\cdot\lambda_p(g,ab),\\
\lambda_p(a,g)\cdot\lambda_p(ag,b) &= \omega(a,g,b)\cdot^a \lambda_p(g,b)\cdot\lambda_p(a,gb).
\end{aligned} \tag{C7}$$

Writing Eq. (C7) in a more convenient way (we ignore the subscript p henceforth):

$$\begin{aligned}
\omega(a,b,g) &= \lambda^{-1}(a,bg)\cdot^{W_a a}\lambda^{-1}(b,g)\cdot\lambda(a,b)\cdot\lambda(ab,g),\\
\omega(g,a,b) &= \lambda^{-1}(g,ab)\cdot^{W_g g}\lambda^{-1}(a,b)\cdot\lambda(g,a)\cdot\lambda(ga,b),\\
\omega^{-1}(a,g,b) &= \lambda^{-1}(ag,b)\lambda^{-1}(a,g)\cdot^{W_a a}\lambda(g,b)\cdot\lambda(a,gb).
\end{aligned} \tag{C8}$$

We have

$$\begin{aligned}
&\delta_g^\omega(a,b) = [\omega(g,a,b)]\cdot[\omega^{-1}(a,g,b)]\cdot[\omega(a,b,g)]\\
&= \lambda^{-1}(g,ab)\cdot^{W_g g}\lambda^{-1}(a,b)\cdot[\lambda(g,a)\cdot\lambda^{-1}(a,g)]\\
&\cdot^{W_a a}[\lambda(g,b)\cdot\lambda^{-1}(b,g)]\cdot\lambda(a,b)\cdot\lambda(ab,g)
\end{aligned} \tag{C9}$$

We can simplify Eq. (C9) by defining ${}^{W_g g}W_a a = \xi_a(g) W_a a, a \in G$, where $\xi_a(g) = \prod \lambda_a(g)$. Another way of computing $\xi_a(g)$ is

$$\begin{aligned}
&\xi_a(g) = W_g g W_a a (W_g g)^{-1}(W_a a)^{-1} = \eta(g,a)\eta^{-1}(a,g)\\
&\to \lambda_a(g) = \lambda(g,a)\lambda^{-1}(a,g).
\end{aligned} \tag{C10}$$

Then Eq. (C9) becomes

$$\lambda_a(g)\cdot^{W_a a}\lambda_b(g) = \delta_g^\omega(a,b)\cdot^{W_g g}\lambda(a,b)\cdot\lambda_{ab}(g)\cdot\lambda^{-1}(a,b). \tag{C11}$$

Appendix D: The projective representation carried by a g-symmetry-defect

In this section we want to give a tensor proof of the following fact[50]: for an SPT state characterized by the 3-cocycle $\omega(a,b,c) \in H^3(G,U(1))$, the projective representation carried by the symmetry g-defect is represented by the inverse of the slant product $[\delta_g^\omega(a,b)]^{-1}$.

To this end, we first create an open g-defect string with a pair of g-defects on the two ends in the given ground-state SPT wave-function $|\Psi\rangle$. The wave-function is denoted as $|\Psi_{defect}\rangle$. This is done in the tensor language

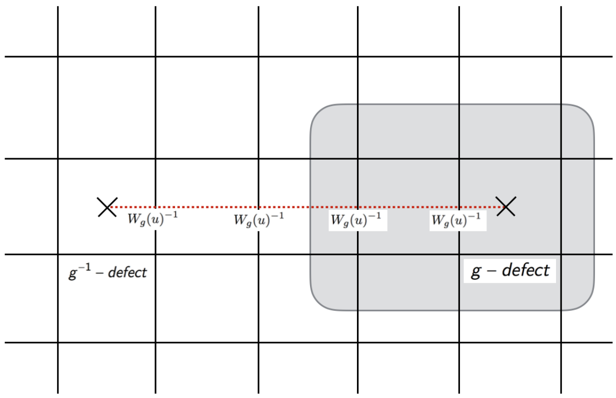

FIG. 7: An example of g-defect line. The g-defect line is obtained by inserting W_g on only one side of the virtual legs crossed by the red dashed line. The tensors close to the defect core should be revised in order to make the tensor wave-function symmetric and non-vanishing. Following the usual convention, we say that the defect line always points from g^{-1}-defect to g-defect, and we always insert W_g to the left when one goes forward along the line. Therefore in the figure we can identify the right end as the g-defect (remember $W_g(d) = W_g(u)^{-1}$). The grey area encloses a g-defect and we can to measure its projective representation through the action of $\eta'(a,b)$ on the boundary virtual legs, see the discussion in the main text.

by inserting W_g strings and modifying the tensors close to the defect core as shown in Fig. 7.

Let's take a patch enclosing one of the two g-defects and measure the projective representation carried by the g-defect. Before the insertion of the g-defect, the local symmetry action $U(a)$ on the patch is defined as acting W_a on the virtual legs on the edge and $D(a)$ on the physical legs inside the patch, *i.e.*,

$$U(a) = \prod_{\text{boundary}} W_a \prod_{\text{bulk}} D(a). \tag{D1}$$

The symmetry operation should leave $|\Psi\rangle$ invariant up to a phase. Then the projective representation inside the patch is measured by acting

$$D(a) \cdot D(b) \cdot [D(a \circ b)]^{-1} \tag{D2}$$

on the physical legs inside the patch. Alternatively, we can do this by monitoring the inverse of the phase generated by acting $\eta(a,b) \equiv W_a \cdot {}^a W_b \cdot (W_{ab})^{-1}$ on the boundary virtual legs since, by our assumption, the action of $U(a)U(b)U(ab)^{-1}$ leaves the patch fully invariant.

In general , acting $\eta(a,b)$ on the virtual legs of a tensor leaves the tensor invariant only up to a phase. Therefore η itself is not a global IGG. Instead, we have

$$\eta(a,b) = W_x(a,b)\eta'(a,b), \tag{D3}$$

where $W_x(a,b)$ is a pure-phase gauge transformation which yields the extra phase for each site and $\eta'(a,b)$ leaves every tensor invariant. Now $\eta'(a,b)$ is decomposable and we denote it as $\eta'(a,b) = \prod \lambda_p(a,b)$.

As for our present case, suppose we have the action of $\prod_{\text{boundary}} \eta(a,b)$ on the ground state wave-function

$$\prod_{\text{boundary}} \eta(a,b) |\Psi\rangle = e^{i\phi} |\Psi\rangle\,, \tag{D4}$$

from which we know that the projective representation inside the patch is just $\prod_{\text{bulk}}(D(a) \cdot D(b) \cdot [D(a \circ b)]^{-1}) = e^{-i\phi}$.

From the previous discussion we have

$$e^{-i\phi} \prod_{\text{boundary}} \eta(a,b) = \prod_{\text{boundary}} \eta'(a,b). \tag{D5}$$

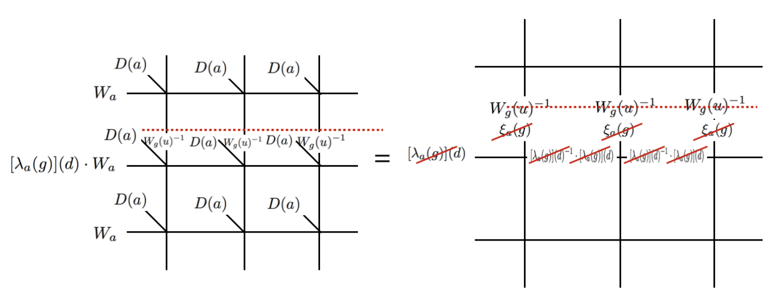

FIG. 8: Invariance of the wave-function under $U^g(a)$. In the figure we can see that $\tilde{W}_a = [\lambda_a(g)](d) \cdot W_a$ where the defect line crosses the boundary and $\tilde{W}_a = W_a$ elsewhere. Such a definition ensures that no boundary excitations are created by acting $U^g(a)$ (for the moment we do not care about what happens at the defect core). In deriving the second figure, we have used the invariance of the tensor under $W_a a$, the identity $W_a W_g^{-1} = W_g^{-1} \xi_a(g) W_a$ and invariance of the tensor under plaquette IGG $\lambda_a(g)$.

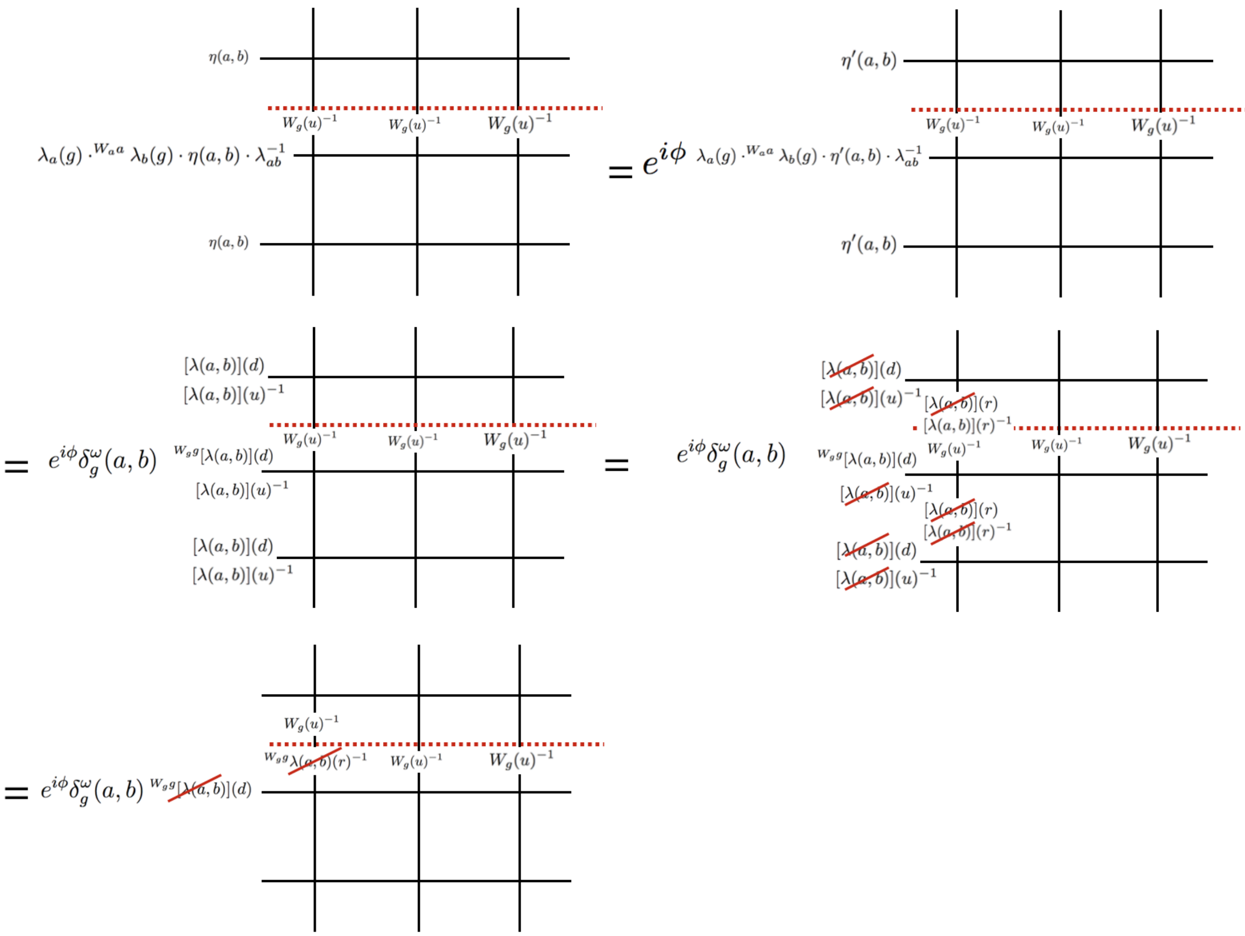

FIG. 9: Measurement of projective representation carried by g-defect. From Eq. (D6), we know that $\tilde{\eta}(a,b) = \lambda_a(g) \cdot^{W_a a} \lambda_b(g) \cdot \eta(a,b) \cdot \lambda_{ab}^{-1}$ where the boundary is crossed by the defect line and $\tilde{\eta}(a,b) = \eta(a,b)$ elsewhere. In the first equality we have used Eq. (D5). In the second equality we have used the decomposition of $\eta'(a,b)$ and Eq. (C11). In the third equality we have used the tensor invariance under plaquette IGG. In the last equality we have used the identity $\lambda(r)^{-1} \cdot W_g^{-1} = W_g^{-1} \cdot^{W_g} \lambda(r)^{-1}$ and the tensor invariance under plaquette IGG.

After the insertion of g-defect, the new local symmetry operation $U^g(a)$ should be defined as acting $\tilde{W}_a$ on the virtual legs on the edge and $D(a)$ on the physical legs inside the patch. Here we have used the $\tilde{W}_a$ as shown in Fig. 8 where $\tilde{W}_a$ on the bond crossing the defect line is changed to be $[\lambda_a(g)](d) \cdot W_a$ and remains W_a elsewhere. This newly-defined $\tilde{W}_a$ ensures that no boundary excitations are created. The physical symmetry operation in the bulk should still be the same.

We will then use $\prod_{\text{boundary}} \tilde{\eta}(a,b)$ to measure the projective representation inside the patch, where $\tilde{\eta}(a,b) \equiv \tilde{W}_a \cdot^a \tilde{W}_b \cdot (\tilde{W}_{ab})^{-1}$. Far away from the defect core, the tensor wave-function is basically the same as before. And $\prod_{\text{boundary}} \tilde{\eta}(a,b)$ will be the same as $\prod_{\text{boundary}} \eta(a,b)$ except at the bond crossing the defect line, see Fig. 9. The $\tilde{\eta}(a,b)$ at the bond crossing the defect line should be $\tilde{W}_a \cdot^a \tilde{W}_b \cdot (W_{ab})^{-1}$:

$$\begin{aligned}
&[\lambda_a(g)](d) \cdot W_a \cdot^a [\lambda_b(g)](d) \cdot^a W_b \cdot ([\lambda_{ab}(g)](d) \cdot W_{ab})^{-1} \\
&= [\lambda_a(g)](d) \cdot^{W_a a} [\lambda_b(g)](d) \cdot W_a \cdot^a W_b \cdot (W_{ab})^{-1}[\lambda_{ab}^{-1}(g)](d) \\
&= [\lambda_a(g)](d) \cdot^{W_a a} [\lambda_b(g)](d) \cdot \eta(a,b) \cdot [\lambda_{ab}^{-1}(g)](d).
\end{aligned} \tag{D6}$$

We can work with the decomposable $\eta'(a,b)$ at the boundary if we keep track of the $e^{i\phi}$ phase. After going through the calculation as shown in Fig. 9, we have

$$\prod_{bdr} \tilde{\eta}(a,b) \left|\Psi_{defect}\right\rangle = e^{i\phi}\delta_g^\omega(a,b) \left|\Psi_{defect}\right\rangle. \tag{D7}$$

Comparing Eq. (D4) with Eq. (D7) and note that projective representation is defined through the inverse of Eq. (D4), we know that the g-defect carries $[\delta_g^\omega(a,b)]^{-1}$ projective representation.

Appendix E: Consequence of the magnetic translation symmetry in tensor-network formulation

The magnetic translation symmetry and on-site projective representation constrain the possible symmetric short-range entangled states in a system. Specifically, we have the following fact: for a system with on-site projective representation of the on-site symmetry group G characterized by $\alpha(a,b)$ and magnetic translation symmetry $T_xT_yT_x^{-1}T_y^{-1}=g$, an SPT ground state described by the 3-cocycle $\omega\in H^3(G,U(1))$ can be realized as its ground state only when $\delta_g^{\omega}(a,b)=\alpha(a,b)^{-1}$.

1. Basic set-up

We have $T_xT_yT_x^{-1}T_y^{-1}=g$, which leads to

$$W_{T_x}T_xW_{T_y}T_y(W_{T_x}T_x)^{-1}(W_{T_y}T_y)^{-1}=W_gg. \tag{E1}$$

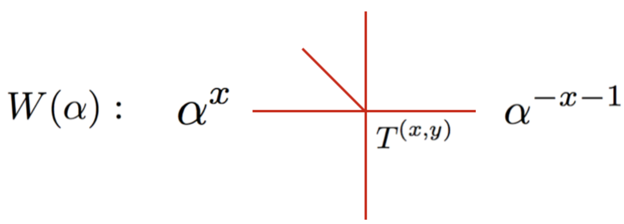

FIG. 10: The definition of phase-gauge transformation $W(\alpha(a,b))$.

We define $\eta(a,b)$ as

$$W_a\cdot^{a}W_b=\eta(a,b)W_{ab}. \tag{E2}$$

By acting $\eta(a,b)$ on $\mathbb{T}$, we will get an extra phase $\alpha(a,b)^{-1}$ per unit-cell, therefore it is not a global IGG. However, we can define a pure-phase gauge transformation $W(\alpha(a,b))$ which yields exactly the phase $\alpha(a,b)^{-1}$ for every site tensor, see Fig. for an illustration.

Then we can write $\eta(a,b)$ as

$$\eta(a,b)=W(\alpha(a,b))\eta'(a,b), \tag{E3}$$

where $\eta'(a,b)=\prod\lambda(a,b)$ is an IGG and is decomposable.

Similarly since we have $D(g)\circ D(a)=\gamma_a(g)D(a)\circ D(g)$ on physical leg, where $\gamma_a(g)=\alpha(g,a)/\alpha(a,g)\in H^1(G,U(1))$. We write the action of W_gg on W_aa as

$$^{W_gg}W_aa=W(\gamma_a(g))\xi_a(g)\cdot W_aa, \tag{E4}$$

where $\xi_g(a)=\prod\lambda_g(a)$ is a decomposable IGG element and the definition of $W(\gamma_a(g))$ is the same as $W(\alpha(a,b))$.

And as for T_x,T_y, we have

$$^{W_{T_x}T_x}W_aa=W(\gamma_a(T_x))\xi_a(T_x)W_aa, etc.. \tag{E5}$$

We act Eq. (E1) on W_aa and obtain an IGG equation

$$^{W_gg}\xi_a^{-1}(T_y)\cdot{}^{W_ggW_{T_y}T_y}\xi_a^{-1}(T_x)\cdot{}^{W_{T_x}T_x}\xi_a(T_y)\cdot\xi_a(T_x)=\xi_a(g), \tag{E6}$$

which, when lift to plaquette IGG, should give us (we have absorbed the phase ambiguity into the definition of $\lambda_a(g)$)

$$^{W_gg}\lambda_a^{-1}(T_y)\cdot{}^{W_ggW_{T_y}T_y}\lambda_a^{-1}(T_x)\cdot{}^{W_{T_x}T_x}\lambda_a(T_y)\cdot\lambda_a(T_x)=\lambda_a(g). \tag{E7}$$

2. Acting W_gg

We first act W_gg on Eq. (E2), then we have

$$\begin{aligned}&^{W_gg}[W_aaW_bb]={}^{W_gg}[\eta(a,b)W_{ab}ab]\\&\Rightarrow W(\gamma_a(g))\cdot^{a}W(\gamma_b(g))\xi_a(g)\cdot^{W_aa}\xi_b(g)\cdot W_aaW_bb\\&={}^{W_gg}\eta(a,b)\cdot W(\gamma_{ab}(g))\xi_{ab}(g)W_{ab}ab,\end{aligned} \tag{E8}$$

which then leads to

$$\xi_a(g)\cdot^{W_aa}\xi_b(g)={}^{W_gg}\eta'(a,b)\cdot\xi_{ab}(g)\cdot\eta'^{-1}(a,b), \tag{E9}$$

where extra phase factors $W(\alpha(a,b))$, $W(\gamma_a(g))$ all cancel.

When lifting Eq. (E9) to plaquette, we have (from Eq. (C11))

$$\lambda_a(g)\cdot^{W_aa}\lambda_b(g)=\delta_g^{\omega}(a,b)\cdot^{W_gg}\lambda(a,b)\cdot\lambda_{ab}(g)\cdot\lambda(a,b)^{-1}. \tag{E10}$$

3. Acting translation

We have another way of deriving Eq. (E10). We first act $W_{T_x}T_x$ on the two sides of Eq. (E2) and obtain an IGG equation,

$$\xi_a(T_x)\cdot^{W_aa}\xi_b(T_x)={}^{W_{T_x}T_x}\eta(a,b)\cdot\xi_{ab}(T_x)\eta(a,b)^{-1}, \tag{E11}$$

where the extra $W(\gamma_a(T_x)),W(\gamma_b(T_x)),W(\gamma_{ab}(T_x))$ cancel since we have $\gamma_a(T_x)\cdot^{a}\gamma_b(T_x)=\gamma_{ab}(T_x)$.

When lift Eq. (E11) to plaquette IGG, we have

$$\lambda_a(T_x)\cdot^{W_aa}\lambda_b(T_x)=[\alpha(a,b)]^{-y}\cdot^{W_{T_x}T_x}\lambda(a,b)\lambda_{ab}(T_x)\lambda^{-1}(a,b), \tag{E12}$$

where $\prod[\alpha(a,b)]^{-y}={}^{W_{T_x}T_x}W(\alpha(a,b))\cdot W(\alpha(a,b))^{-1}$ and the plaquette IGG $[\alpha(a,b)]^{-y}$ are just loops of phases as shown in Fig. 11.

Similarly we have

$$\lambda_a(T_y)\cdot^{W_aa}\lambda_b(T_y)={}^{W_{T_y}T_y}\lambda(a,b)\lambda_{ab}(T_y)\lambda^{-1}(a,b), \tag{E13}$$

where there is no extra factor coming from $^{W_{T_y}T_y}W(\alpha(a,b))\cdot W(\alpha(a,b))^{-1}$ since it is T_y invariant.

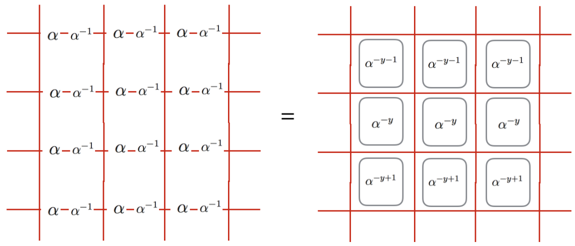

FIG. 11: The decomposition rule of ${}^{W_{T_x}T_x}W(\alpha(a,b))\cdot W(\alpha(a,b))^{-1}$ (LHS) as a product of plaquette IGG $\lambda(\alpha(a,b))$ (RHS).

With Eq. (E12) and Eq. (E13) we can explicitly calculate the action of $W_{T_x}T_xW_{T_y}T_y(W_{T_x}T_x)^{-1}(W_{T_y}T_y)^{-1}$ on Eq. (E2) in terms of plaquette IGG. The action of $W_{T_x}T_xW_{T_y}T_y(W_{T_x}T_x)^{-1}(W_{T_y}T_y)^{-1}$ on LHS of Eq. (E2) is

$$\begin{aligned}
&{}^{W_g g}[\lambda_a(T_y)\cdot^{W_a a}\lambda_b(T_y)]^{-1}\cdot^{W_g gW_{T_y}T_y}[\lambda_a(T_x)^{W_a a}\lambda_b(T_x)]^{-1}\cdot^{W_{T_x}T_x}[\lambda_a(T_y)^{W_a a}\lambda_b(T_y)]\cdot[\lambda_a(T_x)^{W_a a}\lambda_b(T_x)]\\
&={}^{W_g gW_a a}\lambda_b^{-1}(T_y)\cdot^{W_g g}[\lambda_a^{-1}(T_y)\cdot^{W_{T_y}T_yW_a a}\lambda_b^{-1}(T_x)^{W_{T_y}T_y}\lambda_a^{-1}(T_x)]\cdot^{W_{T_x}T_x}\lambda_a(T_y)\cdot^{W_{T_x}T_xW_a a}\lambda_b(T_y)\cdot\lambda_a(T_x)^{W_a a}\lambda_b(T_x)\\
&=\lambda_a(g)^{W_a aW_g g}\lambda_b^{-1}(T_y)\cdot\lambda_a^{-1}(g)\cdot^{W_g g}[{}^{W_a aW_{T_y}T_y}\lambda_b^{-1}(T_x)\lambda_a^{-1}(T_y)^{W_{T_y}T_y}\lambda_a^{-1}(T_x)]\cdot^{W_{T_x}T_x}\lambda_a(T_y)\cdot\lambda_a(T_x)\\
&\cdot^{W_a aW_{T_x}T_x}\lambda_b(T_y)\cdot^{W_a a}\lambda_b(T_x)\\
&=\lambda_a(g)\cdot^{W_a aW_g g}\lambda_b^{-1}(T_y)\cdot^{W_a aW_g gW_{T_y}T_y}\lambda_b^{-1}(T_x)\cdot[\lambda_a^{-1}(g)^{W_g g}\lambda_a^{-1}(T_y)^{W_g gW_{T_y}T_y}\lambda_a^{-1}(T_x)\cdot^{W_{T_x}T_x}\lambda_a(T_y)\lambda_a(T_x)]\\
&\cdot^{W_a aW_{T_x}T_x}\lambda_b(T_y)^{W_a a}\lambda_b(T_x)\\
&=\lambda_a(g)\cdot^{W_a a}[{}^{W_g g}\lambda_b^{-1}(T_y)\cdot^{W_g gW_{T_y}T_y}\lambda_b^{-1}(T_x)\cdot^{W_{T_x}T_x}\lambda_b(T_y)\lambda_b(T_x)]\\
&=\lambda_a(g)\cdot^{W_a a}\lambda_b(g),
\end{aligned}\tag{E14}$$

where we have used Eq. (E4) and Eq. (E5) in the first three equalities and we have used Eq. (E7) in the last two equalities.

The action of $W_{T_x}T_xW_{T_y}T_y(W_{T_x}T_x)^{-1}(W_{T_y}T_y)^{-1}$ on RHS of Eq. (E2) is

$$\begin{aligned}
&{}^{W_g g}[{}^{W_{T_y}T_y}\lambda(a,b)\lambda_{ab}(T_y)\lambda^{-1}(a,b)]^{-1}\cdot^{W_g gW_{T_y}T_y}[\alpha(a,b)^{-y}\cdot^{W_{T_x}T_x}\lambda(a,b)\lambda_{ab}(T_x)\lambda^{-1}(a,b)]^{-1}\\
&\cdot^{W_{T_x}T_x}[{}^{W_{T_y}T_y}\lambda(a,b)\lambda_{ab}(T_y)\lambda^{-1}(a,b)]\cdot\alpha(a,b)^{-y}\cdot^{W_{T_x}T_x}\lambda(a,b)\lambda_{ab}(T_x)\lambda^{-1}(a,b)\\
&={}^{W_{T_y}T_y}[\alpha(a,b)^{-y}]^{-1}\cdot\alpha(a,b)^{-y}\cdot^{W_g g}\lambda(a,b)^{W_g g}\lambda_{ab}^{-1}(T_y)\cdot^{W_g gW_{T_y}T_y}\lambda_{ab}^{-1}(T_x)\cdot^{W_{T_x}T_x}\lambda_{ab}(T_y)\cdot\lambda_{ab}(T_x)\cdot\lambda^{-1}(a,b)\\
&=\alpha(a,b)^{-1}\cdot^{W_g g}\lambda(a,b)\cdot\lambda_{ab}(g)\cdot\lambda^{-1}(a,b),
\end{aligned}\tag{E15}$$

where we have used Eq. (E7) and $\alpha^{-1}(a,b)$ is just a plaquette IGG with loop of phases $\alpha^{-1}(a,b)$.

Combining Eq. (E14) with Eq. (E15), we have

$$\lambda_a(g)\cdot^{W_a a}\lambda_b(g)=\alpha^{-1}(a,b)^{W_g g}\lambda(a,b)\cdot\lambda_{ab}(g)\cdot\lambda^{-1}(a,b).\tag{E16}$$

Comparing Eq. (E16) with Eq. (E10), we have

$$\alpha^{-1}(a,b)=\delta_g^{\omega}(a,b).\tag{E17}$$

It is easy to see that the global phase ambiguities in Eq. (E7),(E12),(E13) will at most modify the LHS of Eq. (E17) up to a 2-cobounday, therefore it should be understood as the 2-cycle equivalence $\delta_g^{\omega}\simeq\alpha^{-1}\in H^2(G,U(1))$.

Appendix F: Generic constructions of symmetry-enforced SPT tensor-network wavefunctions

In this section we want to construct an SPT state with on-site symmetry group G, magnetic translation symmetry satisfying $T_xT_yT_x^{-1}T_y^{-1}=g$ where the SPT is characterized by the 3-cocycle $\omega\in H^3(G,U(1))$ and the on-site symmetry group is represented projectively with the 2-cocycle $\alpha(a,b)$ equal to the inverse of the slant product of ω with respect to g,*i.e.*,

$$\alpha(a,b)\simeq[\delta_g^{\omega}(a,b)]^{-1}\in H^2(G,U(1)).\tag{F1}$$

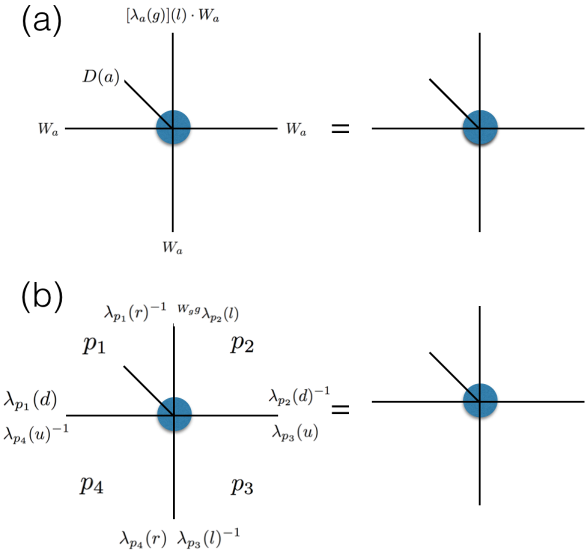

FIG. 12: The original tensor before insertion of g-defect is required to be invariant under the revised symmetry operation and the revised plaquette IGG.

To achieve this goal, we will use the tensor network formalism. Let's start from a SPT tensor wavefunction with the symmetry group $\mathbb{Z}^2 \times G$ described by a 3-cocycle $\omega \in H^3(G, U(1))$, where $\mathbb{Z}^2$ represents the usual translation $T_x^{orig.}, T_y^{orig.}$. Then we know that every tensor is invariant under the action $D(a)$ on physical leg together with $\prod W_a$ on all the virtual legs, from which we have a set of tensor equations. Here we require $D(a)$ to be a direct sum of usual representation $D_1(a)$ and projective representation $D_2(a)$ with 2-cocycle $[\delta_g^\omega(a,b)]^{-1}$. We choose the gauge transformation $W_{T_x^{orig.}}, W_{T_y^{orig.}}$ to be identity for simplicity. The global IGG $\eta(a,b)$ comes from the following tensor equation:

$$W_a \cdot^a W_b = \eta(a,b) W_{ab}, \tag{F2}$$

where $\eta(a,b)$ is decomposable, *i.e.*, $\eta(a,b) = \prod \lambda_p(a,b)$. We require tensors to be fully invariant under $\eta(a,b)$ without even generating phases. This condition ensures $D(a)$ on the physical legs to be projected onto $D_1(a)$ sector.

We define ${}^{W_g g}W_a a = \xi_a(g) W_a a$, where $\xi_a(g) = \prod \lambda_a(g)$ is a decomposable global IGG. More generally we define ${}^{(W_g g)^x}W_a = \xi_a(g,x) W_a$, where $\xi_a(g,x) = \prod \lambda_a(g,x)$. Then we have the following relation:

$$\lambda_a(g, x+1) = {}^{W_g g} \lambda_a(g,x) \cdot \lambda_a(g). \tag{F3}$$

Then we change our tensor wave-function in the following way:

1. We revise the original tensor such that it is invariant under the symmetry operation and the new plaquette IGG defined in Fig. 12. Note that this step is necessary for us to obtain a symmetric and non-vanishing tensor wave-function after the insertion of W_g.

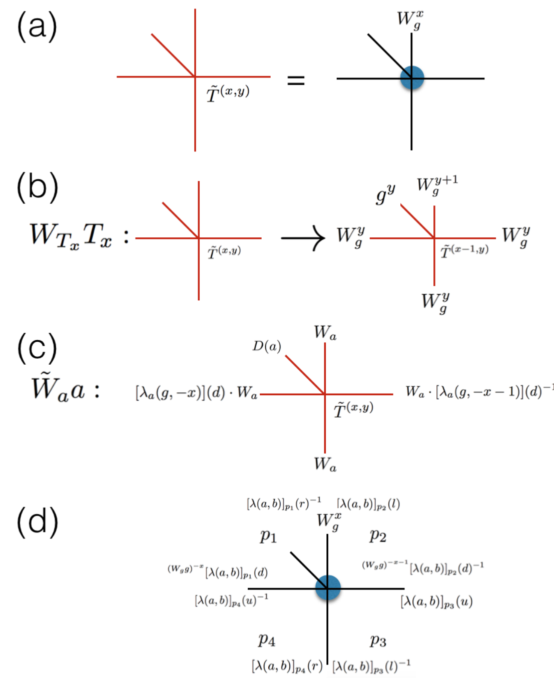

FIG. 13: (a) The definition of the new tensor $\tilde{T}^{(x,y)}$ after the insertion of $[W_g(u)]^x$ to the upper leg of every original tensor $T^{(x,y)}$. (b) The new translation operation $W_{T_x}T_x$. It can be readily checked that $\tilde{T}^{(x,y)}$ is invariant under such translation. Note that we have $T_x = g^y T_x^{orig.}$, $T_y = T_y^{orig.}$ and $W_{T_y} = \mathbf{1}$. (c) The new on-site symmetry operation $\tilde{W}_a a$. It is shown in Fig. 14 that $\tilde{T}^{(x,y)}$ is invariant under such symmetry operation. (d) The new plaquette IGG for the new tensor $\tilde{T}^{(x,y)}$. As before, λ's from different plaquettes commute with each other, and the action of any two λ's in the same plaquette leave the tensor invariant. The tensor $\tilde{T}^{(x,y)}$ invariance under plaquette IGGs follows trivially from Fig. 12.

2. We insert $[W_g(u)]^x$ on the upper leg of every tensor as shown in Fig. 13. Physically it means inserting one g-defect per unit-cell.

3. We define the new on-site symmetry operation $\tilde{W}_a$ and translation symmetry W_{T_x} as shown in Fig. 13. We will show that the new tensor is invariant under such symmetry transformations.

From the last section we have shown that every g-defect carries a projective representation represented by $\delta_g^\omega(a,b)^{-1}$, therefore one would expect after insertion of g-defects, we now have one $\delta_g^\omega(a,b)^{-1}$ projective representation per unit-cell. Let's show it more clearly through explicit calculations.

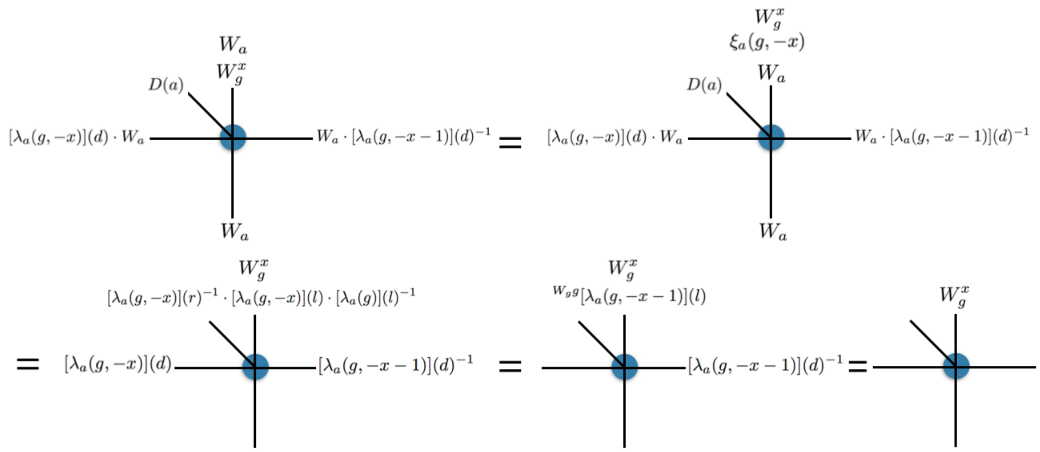

FIG. 14: The revised tensor $\tilde{T}(x,y)$ is invariant under the newly-defined symmetry operation. The first equality comes from the commutation relation $W_aW_g^x = W_g^x\xi_a(g,-x)W_a$. In the second equality we have used the invariance of tensor under W_a as shown in Fig. 12 and the decomposition of $\xi_a(g,-x)$. In the third equality we have used the identity $\lambda_a(g,-x)(l) = {}^{W_g g}[\lambda_a(g,-x-1)](l)\cdot\lambda_a(g)(l)$. And we have also used the invariance of tensor under plaquette IGG as in Fig. 13 in the third and fourth equalities.

First, let's show that the revised tensor wave-function satisfies all the required symmetries. It's apparent that the new tensor has magnetic translation symmetry $W_{T_x}T_x, W_{T_y}T_y$ defined in Fig. 13, *i.e.*

$$W_{T_x}T_xW_{T_y}T_y(W_{T_x}T_x)^{-1}(W_{T_y}T_y)^{-1} = W_g g. \tag{F4}$$

It can be proven that the new tensor is invariant under the new symmetry transformation $\tilde{W}_a a$ as shown in Fig. 14. The invariance of the new tensor $\tilde{T}^{(x,y)}$ under the new plaquette IGG is also apparent as shown in Fig. 13. Then we know that Eq. (C5) still holds for this state, which means the new state obtained is still an SPT state described by the same 3-cocycle ω.

Finally we want to show that the new tensor now carries a projective representation $[\delta_g^\omega(a,b)]^{-1}$ per unit-cell. It can be proven that by acting $\tilde{W}_a \cdot^a \tilde{W}_b\cdot\tilde{W}_{ab}^{-1}$ on all the virtual legs of a tensor we will get a phase $\delta_g^\omega(a,b)$ for every tensor as shown in Fig. 15.

In doing so we need the following identity

$$\lambda_a(g,x)^{W_a a}\lambda_b(g,x)\lambda(a,b)\lambda_{ab}(g,x)^{-1}\cdot^{(W_g g)^x}[\lambda(a,b)^{-1}] = [\delta_g^\omega(a,b)]^x. \tag{F5}$$

Let's denote the LHS of Eq. (F5) as $f(x)$. From Eq. (C11) we have $f(1) = \delta_g^\omega(a,b)$, then we need to find out the relation between $f(x)$ and $f(x+1)$. Using $\lambda(g,x) = {}^{W_g g}\lambda(g,x-1)\cdot\lambda(g)$, we can rewrite Eq. (F5) as

$$\begin{aligned}
&[{}^{W_g g}\lambda_a(g,x-1)\lambda_a(g)]^{W_a a}[{}^{W_g g}\lambda_b(g,x-1)\cdot\lambda_b(g)]\lambda(a,b)[{}^{W_g g}\lambda_{ab}(g,x-1)\cdot\lambda_{ab}(g)]^{-1}\cdot^{(W_g g)^x}[\lambda(a,b)^{-1}]\\
&= [{}^{W_g g}\lambda_a(g,x-1)\lambda_a(g)]^{W_a a W_g g}\lambda_b(g,x-1)\cdot^{W_a a}\lambda_b(g)\lambda(a,b)\lambda_{ab}(g)^{-1}\cdot[{}^{W_g g}\lambda_{ab}(g,x-1)]^{-1}\cdot^{(W_g g)^x}[\lambda(a,b)^{-1}]\\
&= {}^{W_g g}\lambda_a(g,x-1)[\lambda_a(g)\xi_a^{-1}(g)]^{W_g g W_a a}\lambda_b(g,x-1)\xi_a(g)^{W_a a}\lambda_b(g)\lambda(a,b)\lambda_{ab}(g)^{-1}\cdot^{W_g g}[\lambda_{ab}(g,x-1)]^{-1}\cdot^{(W_g g)^x}[\lambda(a,b)^{-1}]\\
&= \delta_g^\omega(a,b)^{W_g g}\lambda_a(g,x-1)[\lambda_a(g)\xi_a^{-1}(g)]^{W_g g W_a a}\lambda_b(g,x-1)[\xi_a(g)\lambda_a(g)^{-1}]^{W_g g}\lambda(a,b)\cdot^{W_g g}[\lambda_{ab}(g,x-1)]^{-1}\cdot^{(W_g g)^x}[\lambda(a,b)^{-1}]\\
&= \delta_g^\omega(a,b)^{W_g g}[\lambda_a(g,x-1)^{W_a a}\lambda_b(g,x-1)\lambda(a,b)\cdot\lambda_{ab}(g,x-1)^{-1}\cdot^{(W_g g)^{x-1}}\lambda(a,b)^{-1}].
\end{aligned} \tag{F6}$$

The above derivation tells us that $f(x) = \delta_g^\omega(a,b)^{W_g g}f(x-1)$, therefore by induction we have $f(x) = [\delta_g^\omega(a,b)]^x$.

With the help of Eq. (F5), we can readily calculate the new IGG $\tilde{\eta}(a,b) \equiv \tilde{W}_a\cdot^a\tilde{W}_b\cdot\tilde{W}_{ab}^{-1}$. The $\tilde{\eta}(a,b)$ on the up

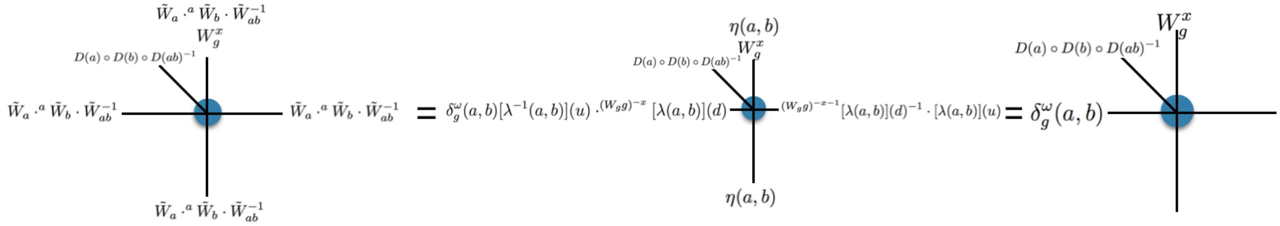

FIG. 15: Every site-tensor carries a projective representation characterized by $[\delta_g^\omega(a,b)]^{-1}$. We show this by acting $\tilde{W}_a a \tilde{W}_b b(\tilde{W}_{ab} ab)^{-1}$ on both the physical legs and the virtual legs of tensor $\tilde{T}^{(x,y)}$, which should leave the tensor invariant without generating any phase. But from the calculation we find that the action on vitrual legs will contribute a factor $\delta_g^\omega(a,b)$, therefore the representation on the physical legs are $D(a)\cdot D(b) = [\delta_g^\omega(a,b)]^{-1} D(ab)$, *i.e.*, they are projected onto the $D_2(a)$ sector with projective representation. In the calculation above, we have used Eq. (F5) in the first equality. And we have used the invariance of the tensor under the plaquette IGG defined in Fig. 13 in the second equality.

and down virtual legs are just $\eta(a,b)$ defined before. The $\tilde{\eta}(a,b)$ on the left leg is computed as follows:

$$\begin{aligned}
&[\lambda_a(g,-x)](d)\cdot W_a \cdot^a [\lambda_b(g,-x)](d) \cdot^a W_b \cdot ([\lambda_{ab}(g,-x)](d)\cdot W_{ab})^{-1} \\
&= [\lambda_a(g,-x)](d) \cdot^{W_a a} [\lambda_b(g,-x)](d) \cdot W_a \cdot^a W_b \cdot (W_{ab})^{-1} [\lambda_{ab}(g,-x)](d)^{-1} \\
&= [\lambda_a(g,-x)](d) \cdot^{W_a a} [\lambda_b(g,-x)](d) \cdot \eta(a,b) \cdot [\lambda_{ab}(g,-x)](d)^{-1} \\
&= [\delta_g^\omega(a,b)]^{-x} [\lambda(a,b)](u)^{-1} \cdot^{(W_g g)^{-x}} [\lambda(a,b)](d).
\end{aligned} \tag{F7}$$

Similarly, we have on the right leg

$$[\delta_g^\omega(a,b)]^{x+1} \cdot^{(W_g g)^{-x-1}} [\lambda(a,b)](d)^{-1} \cdot [\lambda(a,b)](u). \tag{F8}$$

Therefore, as shown in Fig. 15, we know that $\tilde{\eta}(a,b)$ is just $\delta_g^\omega(a,b)$ times the product of plaquette IGG shown in Fig. 13 which leaves the tensor invariant up to a phase $\delta_g^\omega(a,b)$. Then on the physical leg we are forced to have $D(a)D(b) = [\delta_g^\omega(a,b)]^{-1} D(ab)$, *i.e.*, $D(a)$ is projected onto $D_2(a)$ sector. So the desired on-site projective representation is achieved.

[1] E. Lieb, T. Schultz, and D. Mattis, Annals of Physics **16**, 407 (1961).
[2] M. Oshikawa, Phys. Rev. Lett. **84**, 1535 (2000).
[3] A. Paramekanti and A. Vishwanath, Phys. Rev. B **70**, 245118 (2004).
[4] M. B. Hastings, Physical review b **69**, 104431 (2004).
[5] M. B. Hastings, EPL (Europhysics Letters) **70**, 824 (2005).
[6] M. P. Zaletel and A. Vishwanath, Physical review letters **114**, 077201 (2015).
[7] M. Cheng, M. Zaletel, M. Barkeshli, A. Vishwanath, and P. Bonderson, arXiv preprint arXiv:1511.02263 (2015).
[8] X.-L. Qi and S.-C. Zhang, Rev. Mod. Phys. **83**, 1057 (2011).
[9] M. Z. Hasan and C. L. Kane, Rev. Mod. Phys. **82**, 3045 (2010).
[10] I. Affleck, T. Kennedy, E. H. Lieb, and H. Tasaki, Phys. Rev. Lett. **59**, 799 (1987).
[11] X. Chen, Z.-C. Gu, Z.-X. Liu, and X.-G. Wen, Science **338**, 1604 (2012), http://science.sciencemag.org/content/338/6114/1604.full.pdf.
[12] X. Chen, Z.-C. Gu, Z.-X. Liu, and X.-G. Wen, Phys. Rev. B **87**, 155114 (2013).
[13] I. Dana, Y. Avron, and J. Zak, Journal of Physics C: Solid State Physics **18**, L679 (1985).
[14] Y.-M. Lu, Y. Ran, and M. Oshikawa, arXiv preprint arXiv:1705.09298 (2017).
[15] J. Wu, T.-L. Ho, and Y.-M. Lu, arXiv preprint arXiv:1703.04776 (2017).
[16] D.-H. Lee and M. P. Fisher, Physical review letters **63**, 903 (1989).
[17] Y.-M. Lu and A. Vishwanath, Phys. Rev. B **93**, 155121 (2016).
[18] T. Senthil and M. Levin, Phys. Rev. Lett. **110**, 046801 (2013).
[19] L. Balents, M. P. Fisher, and C. Nayak, Physical Review B **60**, 1654 (1999).
[20] X.-G. Wen, *Quantum field theory of many-body systems: from the origin of sound to an origin of light and electrons*

(Oxford University Press on Demand, 2004).
[21] S. Jiang and Y. Ran, Physical Review B **95**, 125107 (2017).
[22] K. Duivenvoorden, M. Iqbal, J. Haegeman, F. Verstraete, and N. Schuch, arXiv preprint arXiv:1702.08469 (2017).
[23] L. Balents, M. P. A. Fisher, and S. M. Girvin, Phys. Rev. B **65**, 224412 (2002).
[24] D. Sheng and L. Balents, Physical review letters **94**, 146805 (2005).
[25] S. Isakov, Y. B. Kim, and A. Paramekanti, Physical review letters **97**, 207204 (2006).
[26] X.-G. Wen, Phys. Rev. B **65**, 165113 (2002).
[27] A. Kitaev, Annals of Physics **321**, 2 (2006).
[28] A. Mesaros and Y. Ran, Phys. Rev. B **87**, 155115 (2013).
[29] M. Barkeshli, P. Bonderson, M. Cheng, and Z. Wang, arXiv preprint arXiv:1410.4540 (2014).
[30] J. B. Kogut, Reviews of Modern Physics **51**, 659 (1979).
[31] D. S. Rokhsar and S. A. Kivelson, Physical review letters **61**, 2376 (1988).
[32] SPT phases protected by $G = SO(3) \times Z_2^{Ising}$ form a group $H^3(SO(3) \times Z_2^{Ising}, U(1))$. The Kunneth formula gives: $H^3(SO(3) \times Z_2^{Ising}, U(1)) = H^3(SO(3), U(1)) \times H^3(Z_2, U(1)) \times H^2(SO(3), Z_2) = Z \times Z_2 \times Z_2$. Following the Remark, it is straightforward to show that only the Z_2 index in $H^2(SO(3), Z_2)$ is enforced to be nontrivial. (Namely ω_0 in Theorem-(2) can be chosen to be the nontrivial element in $H^2(SO(3), Z_2)$,and the kernal $\mathcal{A}_g = H^3(SO(3), U(1)) \times H^2(SO(3), Z_2) = Z \times Z_2$.).
[33] Following the Kunneth formula: $H^3(Z_2^T \times Z_2^{Ising}, U(1)) = H^3(Z_2^T, U(1)) \times H^3(Z_2, U(1)) \times H^2(Z_2^T, Z_2) = Z_1 \times Z_2 \times Z_2$. In this example, the Z_2 index in $H^2(Z_2^T, Z_2)$ is enforced to be nontrivial, and the Z_2 index in $H^3(Z_2, U(1))$ is enforced to be trivial. This is because here ω_0 in Theorem-2 is the nontrivial element in $H^2(Z_2^T, Z_2)$, and the kernel subgroup $\mathcal{A}_g = Z_1$.
[34] X. Chen, Y.-M. Lu, and A. Vishwanath, Nature communications **5** (2014).
[35] R. Moessner and S. L. Sondhi, Phys. Rev. Lett. **86**, 1881 (2001).
[36] Y. Qi, Z.-C. Gu, and H. Yao, Physical Review B **92**, 155105 (2015).
[37] R. Moessner and S. Sondhi, Physical Review B **63**, 224401 (2001).
[38] R. Moessner, S. L. Sondhi, and E. Fradkin, Physical Review B **65**, 024504 (2001).
[39] R. Moessner, S. Sondhi, and P. Chandra, Physical review letters **84**, 4457 (2000).
[40] A. Y. Kitaev, Annals of Physics **303**, 2 (2003).
[41] M. Levin and Z.-C. Gu, Phys. Rev. B **86**, 115109 (2012).
[42] D. Pérez-García, M. Sanz, C. Gonzalez-Guillen, M. M. Wolf, and J. I. Cirac, New Journal of Physics **12**, 025010 (2010).
[43] H. Zhao, Z. Xie, Q. Chen, Z. Wei, J. Cai, and T. Xiang, Physical Review B **81**, 174411 (2010).
[44] S. Singh, R. N. C. Pfeifer, and G. Vidal, Phys. Rev. A **82**, 050301 (2010).
[45] S. Singh, R. N. Pfeifer, and G. Vidal, Physical Review B **83**, 115125 (2011).
[46] S. Singh and G. Vidal, Physical Review B **86**, 195114 (2012).
[47] B. Bauer, P. Corboz, R. Orús, and M. Troyer, Physical Review B **83**, 125106 (2011).
[48] A. Weichselbaum, Annals of Physics **327**, 2972 (2012).
[49] S. Jiang and Y. Ran, Phys. Rev. B **92**, 104414 (2015).
[50] M. P. Zaletel, Physical Review B **90**, 235113 (2014).
[51] F. Pollmann, A. M. Turner, E. Berg, and M. Oshikawa, Phys. Rev. B **81**, 064439 (2010).
[52] X. Chen, Z.-C. Gu, and X.-G. Wen, Phys. Rev. B **83**, 035107 (2011).
[53] S. A. Parameswaran, A. M. Turner, D. P. Arovas, and A. Vishwanath, Nature Physics **9**, 299 (2013).
[54] H. C. Po, H. Watanabe, C.-M. Jian, and M. P. Zaletel, ArXiv e-prints (2017), arXiv:1703.06882 [cond-mat.str-el].
[55] Y.-M. Lu, arXiv preprint arXiv:1705.04691 (2017).